CHALMERS
UNIVERSITY OF TECHNOLOGY

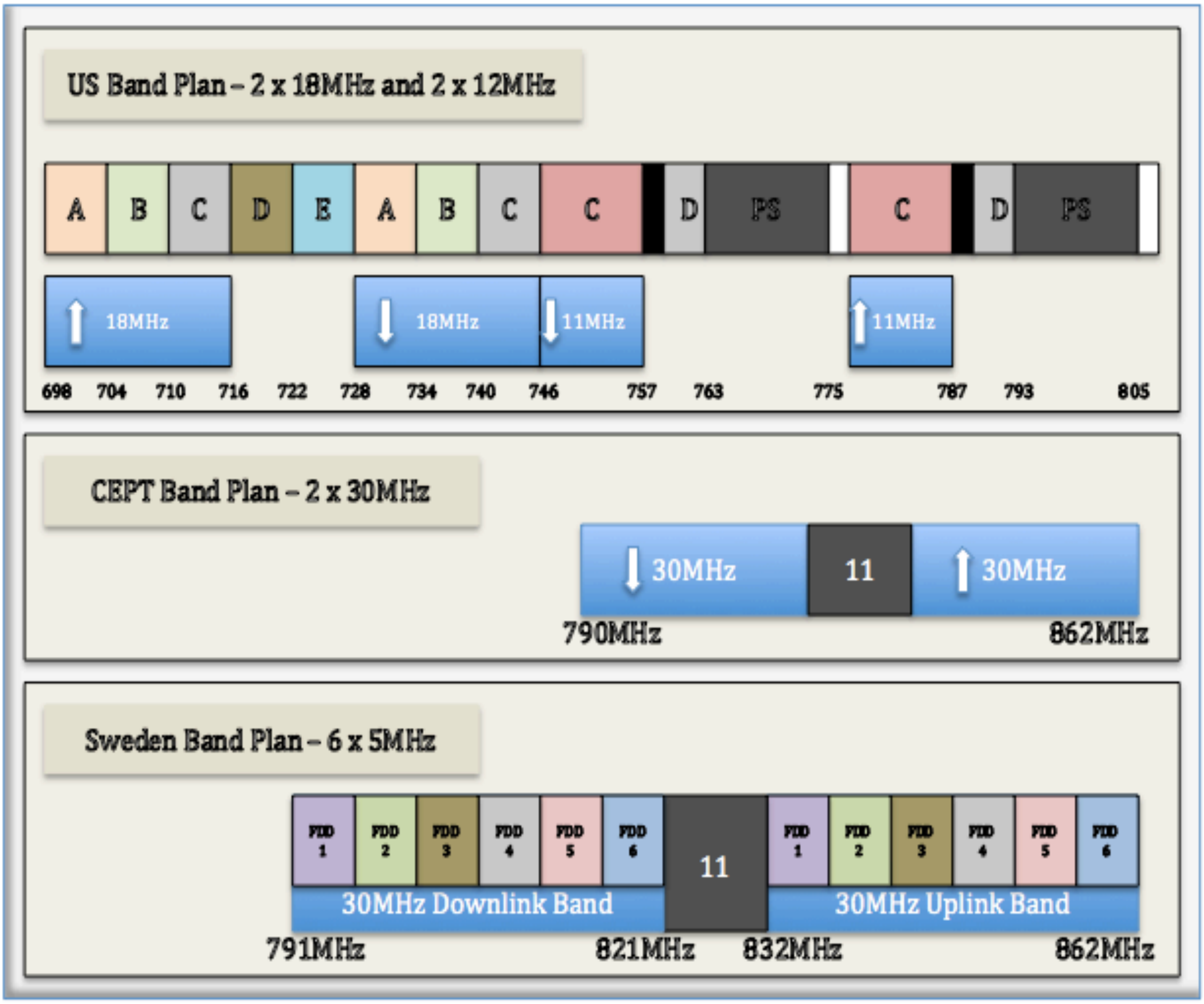

Spectrum Allocation Strategies for Future Wireless Networks

MUHAMMAD HAMMAD SAGHIR

Department of Signals and systems
CHALMERS UNIVERSITY OF TECHNOLOGY
Gothenburg, Sweden 2015

MASTER'S THESIS

Spectrum Allocation Strategies for Future Wireless Networks

MUHAMMAD HAMMAD SAGHIR

CHALMERS
UNIVERSITY OF TECHNOLOGY

Department of Signals and System
CHALMERS UNIVERSITY OF TECHNOLOGY
Gothenburg, Sweden 2015

Spectrum Allocation Strategies for Future Wireless Networks

MUHAMMAD HAMMAD SAGHIR

REPORT NO. EX056/2015

Supervisor: Prof. Tommy Svensson, Department Signals and Systems

Examiner: Prof. Tommy Svensson, Department Signals and Systems

Master’s Thesis
Department of Signals and Systems
Chalmers University of Technology
SE-412 96 Gothenburg
Telephone +46 31 772 1000

Cover: The Digital Dividend (DD) bands

Typeset in MS Word 2011
Gothenburg, Sweden 2015

Spectrum Allocation Strategies for Future Wireless Networks
MUHAMMAD HAMMAD SAGHIR
Department of Signals and Systems
Chalmers University of Technology

Abstract

The world is moving towards a future where it needs enough spectrum to fulfill its ever increasing traffic demands. It is expected that mobile device per capita would increase from 1.05 in 2014 to 1.50 in 2019. Moreover, studies show that wireless mobile data traffic is expected to grow 1000 folds by 2020. It is very likely given the types of advanced devices that are connecting to wireless networks everyday, and whic are capable of running advanced and data heavy applications. So, it is certain that higher capacity demands will increase in recent future.

From the Shannon capacity relation it is known that capacity depends on bandwidth and signal-to-noise ratio. From all the available electromagnetic wavelengths, ITU has divided and allocated microwave bands to cellular mobile services. Apart from allocated bands, ITU is also making efforts to release lower TV bands to mobile services which would be available for provision of basic services in rural areas.

Current cellular systems use lower bands which are already at their limits in providing maximum capacity. So, future systems are investigating higher frequency bands due to higher bandwidth availability to enhance the capacity. Due to regulatory as well as hardware limitations, not all the bandwidth in a band is available to a user, so moving to higher bands alone is not a solution. Therefore, deploying advanced techniques to improve both the cell and user spectral efficiencies is required in order to provide 1000 fold capacity. These advanced techniques, like Carrier Aggregation (CA), MIMO, Heterogeneous Networks, Relay Nodes, CoMP, will improve both the capacity and coverage.

The main focus of this work is to identify frequency bands that are available for mobile cellular services and investigate the bands on the basis of their link budget. To complete the link budget, different parameters are studied and a generic behavior, with respect to frequency, is defined for all those parameters and some real numbers are selected to complete the link budget. The usability of those bands is checked on two performance matrices, cell coverage and capacity.

This study shows that there are lots of unused spectrum available, especially at higher frequencies. Based on link budget analysis, it is investigated that these bands can meet the future demands of a dense urban information society, both in terms of capacity and coverage. This work concludes that, given an acceptable receiving threshold limit, 95% coverage and beyond 1000-fold capacity can be achieved at EHF bands.

Key words: Spectrum, Digital Dividend (DD), TV White Spaces (TVWS), Transmit Power, Path Loss Models, Carrier Aggregation (CA), Heterogenous Networks (HetNets)

Acknowledgements

I would like to dedicate this work to all those who have invested their time in me, especially my supervisor Assoc. Prof. Tommy Svensson. I am thankful to him for giving me opportunities over and over and making me to reach the end of this work. I admire him and respect him for all his support and patience with me. I wish to be working more with him in future.

Along with Tommy Svensson, there is a long list of people whose help made me able to do a good and efficient work. I thank you all, Mikael Coldrey, Christian Fager, Yngve Hamnerius, Ulf Gustavsson, Nima Jamaly, Mattias Thorsell, Tomas Bryllert, Aditya K. Jagannatham, Sui Yutao and all those whose names I could not remember.

In the end I would really like to thank my parents for their love, support and encouragement at everytime. I really missed you and I dedicate all my efforts and hardwork to you.

Shukr Alhamd-u-Lillah for everything!

Muhammad Hammad Saghir, Göteborg September 2015

Contents

List of Figures

List of Tables

Chapter 1

Introduction

In 2014, alone, half a million new mobile devices and connections were added to the grand total of 7.4 billion. The mobile communication, today, is considered as the most rapidly adopted technology in history that has been gradually increasing. The number of mobile cellular users crossed the numbers of terrestrial telephone users in year 2009 and it keeps on growing exponentially since then [1]. From 2009 to 2014, the cellular subscribers have grown from 4.6 billions to 7.4 billions at a compound annual growth rate (CAGR) of 9.98 percent, as shown in figure 1.1 [1]-[5][11]. Although there has been a continuous growth in mobile subscriptions but the market is reaching to a saturation level [5]. In 2014, there were more than 1.05 mobile cellular devices per-capita but due to some rising factors there is a forecast of 1.5 devices/capita by 2019 [11].

Along with cellular adoption, with the introduction of mobile broadband services, usage of internet, especially the mobile-internet, has also grown. In 2014, global penetration rate of internet reached to 40% with Europe leading with 75% penetration rate. According to ITU statistics [1], mobile broadband overtook the fixed broadband in 2008 at 6% global penetration rate. Since then, over the period of last five years, the mobile broadband has shown an impressive growth with CAGR of 28.52% as subscribers have grown from 656 millions in 2009 to almost 2.3 billions in year 2014 [1]-[5].

With increasing number of mobile connected devices, there would be much more bandwidth needed in future to accommodate them. That is one of the reasons to acquire more bandwidth for future systems. According to studies, the wireless mobile data traffic is expected to grow 1000 fold by year 2020 and more likely to grow to 10,000 folds by 2030 [12]-[15]. Looking at the history of data usage and both the current and emerging trends it is expected to grow that much [6]-[11].

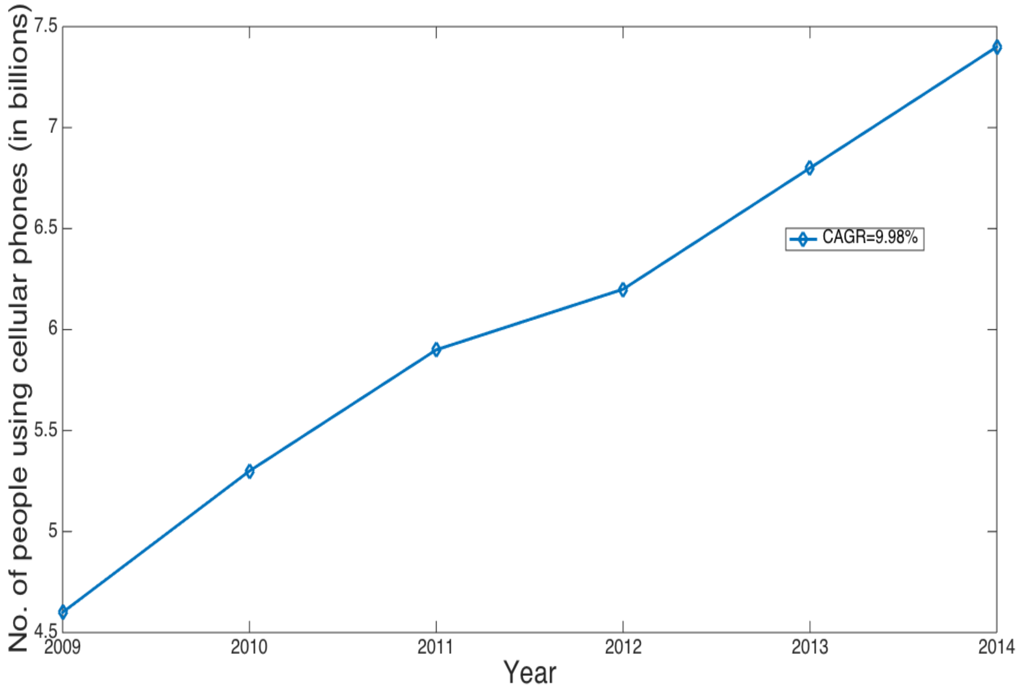

Figure 1.1: Cellular subscriptions growth

1.1 Current and Future Trends

Global mobile data traffic in year 2010 was 237 petabytes per month and reached to 2.5 exabytes (2500 petabytes) per month in 2014 [6,11] with a CAGR of 80.22%. This is interesting to note that the compound growth in mobile broadband is only 23% while traffic growth has been way higher. There are so many different factors that have caused this unusual increase of traffic, like diverse nature of connected devices, types of data services used, advancements in access technology, etc.

1.1.1 Device Growth and Diversification

Mobile devices increase the interaction between a user and network that is likely to increase overall usage resulting into growth of mobile traffic. Each year, various new devices with enhanced intelligence and capabilities are introduced in the market. Studies show that these new smart devices, like smartphones, tablets, laptops, machine-to-machine (M2M), etc. will take over the non-smart devices by the end of year 2016. It is expected that the share of smart devices will rise from 26% in 2014 to around 54% by 2019 [11]. Along with the growth in number, due to their enhanced capabilities these smart devices generate many times more traffic than those non-smart devices. There are many figures quoted in [6]-[11] but the most recent figures are mentioned here in table 1.1 given below. So, by 2019 these smart devices will generate as much as 97% of mobile traffic up from 88% in 2014 [11].

Table 1.1: High-end devices generate significant amount of traffic

Device	Multiple of basic phone data
Smartphone	37 times
Tablet	94 times
Laptop	119 times
M2M Module	3 times
Wearable Device	6 times

Since, according to ITU, the cellular phone adoption is reaching to a saturation level, so the new driving factor to the increase in mobile devices is the M2M, which in general terms is called Internet-of-Everything (IoE). It brings people, processes, data and things together to form a networked society. With the ubiquity of mobile networks, bandwidth intensive M2M applications have become widespread like business and consumer surveillance, eHealthcare systems, telematics, etc. Including the wearable devices, M2M connections are expected to grow from 0.6 billions in 2014 to 3.7 billions in 2019 with CAGR of 44%; among all M2M services healthcare segment is expected to experience highest growth following by automotive industry [8,11].

1.1.2 Trending Services

With increasing numbers of smart devices connecting to mobile network, it is natural to look for the usage trends that affect both the consumer and service provider. In 2013, Cisco did an analysis of what kind of mobile data services are being used the most among 12000 users of their Android based application Data Meter both on smartphones and tablets [9]. The key finding of that analysis was the type of trending application generating the most traffic. The result was no different from previously available records. Almost half of the data consumption between both kinds of users was due to video streaming/communication applications. The results from that study are provided in table 1.2 with other services including.

Mobile video traffic had crossed 50% of the total mobile data traffic for the first time in 2012, 51% to exact [8]. From 2012 to 2014, mobile video traffic grew at 74.54% CAGR while it is expected to grow at 57% CAGR between 2014 and 2019 reaching to 69% of total mobile data traffic as compared to 55% in 2014. There is a forecast on some other trending services, in 2018, by different groups of users in [10].

Table 1.2: Top applications for data consumption [9]

Service	Smartphone (%age of Data Consumption)	Tablet (%age of Data Consumption)
Video/Communication	45%	50%
Information	12%	17%
Web Browsing	6%	7%
Social Networking	7%	3%
Music/Audio Streaming	4%	3%

1.1.3 Advanced Access Technologies

Not only the mobile devices are getting smarter, the access networks are also evolving from lower generation (2G, 3G) to higher generations (3.5G, 4G). These evolved networks are far more intelligent and also faster with higher bandwidth. Although, there is often a delay between two things but there is anecdotal evidence to support the idea that increased speed brings higher usage. The delay is mainly due to the delay in availability of the new technology to potential users.

The service provider can meet the quality of services (QoS) of its consumers by providing higher speed and bandwidth. With higher speed, the average bit rate of content will increase due to smaller latencies. While, as the network capacity increases, operators will more likely introduce appealing broadband packages. Both these things will attract more users and introduction of high capacity services and their adoption will result in more data traffic.

1.2 This Work

All these social developments in inter-connected world will lead to a change how these mobile and wireless communication devices are used. Advent of IoT and other innovative applications will bring more users to the existing system but it will also introduce diversity both in the requirements and the usage scenarios.

More diverse in nature among different scenarios defined in [15] and [16] is a ‘dense urban information society’, where a user is expected to use a diverse range of services and requires the same QoS no matter where they are and what services they are using. This scenario comprised of the requirement of amazingly fast connectivity and great service to highly demanding and diverse crowd, which is usually in the order of 10-100 times the data rate and 1000 times more data volume as of today [15].

The technical challenge is to provide high data rates at application layer with satisfying QoS at a high traffic density per area. The availability of spectrum and its maximum usage efficiency affects the network performance. In order to fulfill these requirements wide carriers are needed along with the technology that can handle these new bands.

1.2.1 Objective

Based on above facts and figures, the purpose of this work is to study and identify the suitable bands to meet both the current and future demands in a highly demanding urban environment. The main objective is to identify all kind of bands available for mobile communication services. For that purpose both the micro-waves and millimeter-waves are studied.

For that wide range of frequencies, lots of parameters needs to be checked on for what values could be used in calculating the link budget. Some regulatory documents and existing systems and their components need to be checked for that purpose.

The link budget draws a rough picture how much basic capacity and coverage is achieved. To complete the picture, some advanced techniques and their respective gains will be studied to achieve the demanded QoS and maximum efficiency of the deployed spectrum. These techniques are deployed at network access layer of TCP/IP protocol.

So, based on the complete analysis of link budget and those techniques, suitable bands will be located for dense urban environment.

1.2.2 Work Outline

In this thesis work, we start from a study survey, where we identify the available mobile-cellular frequency bands and some other bands freed as a result of some developments in recent past. So, chapter 2 discusses the available frequency bands for mobile cellular communication.

The user demands are translated into good coverage and higher capacity. Chapter 3 identifies and defines the important parameters and collects the information to define their numerical values. That is the primary goal of this work. Then these parameters and theirs numbers are used to calculate the link budget for frequency bands listed in chapter 2.

Since, existing systems are not enough to meet the heavy future demands, despite the bandwidth increase. So, some of the techniques, used in LTE-Advanced, to improve both the capacity and coverage are studied and their gains are listed in chapter 4.

Following chapter 4, in chapter 5 we start with discussion on different system parameters we researched. Then we analyze the capacity and coverage obtained as a result of the link budget and added gains of advanced techniques. Then this work is concluded and some future work options are discussed in the end.

Chapter 2

RF Spectrum

Professor and former FCC Commissioner Glen O. Robinson had defined the spectrum as a way of describing the form of electromagnetic (EM) radiations [17]. These electromagnetic radiations have associated wavelengths to them, which could be as high as several kilometers and as low as few pico-meters (10^{-12}). This long list of continuous wavelengths is called the EM spectrum that is divided into several groups, as shown in figure 2.1, depending on the nature and respected wavelengths of the waves.

Existing radio communication systems operate in Radio and Microwave bands, these two bands combined are referred to as RF spectrum. International Telecommunication Union (ITU), a United Nations (UN) telecommunication regulatory body, has divided this RF spectrum into several parts and regulates the use of those small bands for different transmission systems, called Radio Regulations. These regulations also set policies and standards to mitigate the interference among the systems, whether these systems are sharing the same band or sharing the geographical proximity.

ITU has divided the world into three large geographical parts, as shown in figure 2.2, called ITU Regions. The set of regulations may either be same for all or different for different regions or two regions sharing the same regulations in certain bands. Different countries have different national regulatory authorities like Federal Communication Commission (FCC) for US, Swedish Post and Telecom Authority (PTS) for Sweden, etc. These authorities abide by the ITU regulations and implement their policies. To increase the harmony among the countries of a region, some regional authorities, like European Conference of Postal and Telecommunications Administrations (CEPT), make recommendations, which are set forth during the implementation of ITU regulations.

Initially, all three regions had only pre-regulated tables of frequencies and pre-defined frequencies were used for cellular communication. However, due to several recent advancements, some low-end spectrum is being released of other services, which could be useful especially for cellular services. Also, technological advancements have made it

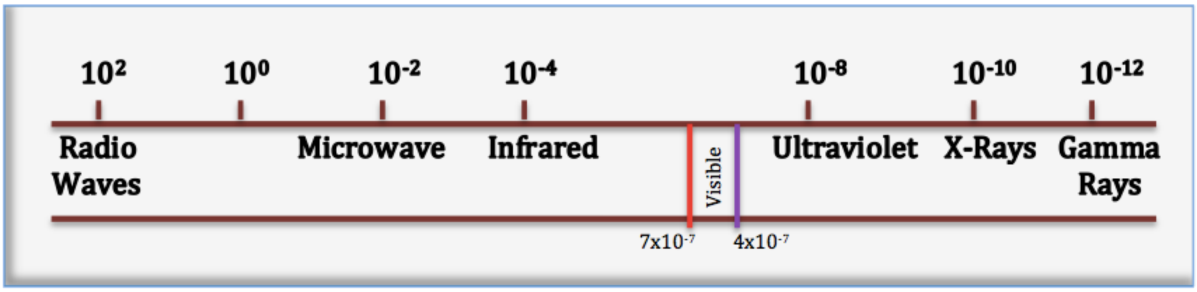

Figure 2.1: Electromagnetic (EM) spectrum

Figure 2.2: ITU regional division

possible to use already allocated, but unused, high-end frequency bands for cellular services. These events would most definitely lead us towards 5th generation of these communication services.

2.1 Regional Allocated Spectrum

The regional frequency allocation tables provide the detailed description of what services could be used in which bands, sometimes many services may share the band. Since, the scope of this study only covers the cellular communications, so only bands used for mobile communications are listed and used for final calculations. Following is the list of bands used for mobile communications in Sweden in table 2.1 [18].

From the table, it can be seen that higher bandwidths are available at the mm-wave frequencies; due to their propagation properties those frequencies are being discussed to use for dense-urban and sub-urban regions to provide high capacity and better coverage by making the cell area smaller. This short coverage limitation along with higher bandwidth provision yields higher spectral efficiency by giving a perfect blend of higher frequency reuse with higher throughputs.

2.2 New Spectrum – Digital Dividend (DD)

During World Radio Conference 2007 (WRC-07), ITU announced to release a good chunk of UHF band, 790-862MHz (called 800MHz band), to be used for mobile services. This spectrum was freed as a result of a decision to switch off the analogue terrestrial services and migrate those programs to digital services. This was all enabled by the pioneering ITU recommendation ITU-R BT.798, which says that digital systems should use same bandwidth as the analogue TVs. Since, the digital compression and multiplexing allows far better utilization of spectrum, a multiple number of programs can be transmitted in the same bandwidth earlier used by a single analogue program, so as a result a lot of spectrum was made free, called Digital Dividend.

At WRC-12, Arab and African countries proposed to release the 694-790MHz bands (called 700MHz band) for mobile services. This spectrum is identified as a potential candidate for second digital dividend but final allocations for this spectrum would be decided at WRC-15 as per request of European countries where this band is still in use of terrestrial TV services.

At WRC-15, there are ten agenda items and number one (1.1–1.18) deals with amending the current radio regulation policies [19]. According to [19], agenda item 1.1 deals with the additional spectrum allocation for IMT and other related regulations, while agenda item 1.2 is subject to examine the results of studies conducted in the 694-790MHz bands for mobile services in region 1.

Rate of deployment of these bands is different in different countries. US lead the world with completing the switchover and auctioning that spectrum for LTE deployment [20]. In US, 800MHz band is utilized by other services, mainly the Public Safety services, but the 700MHz band has already been auctioned; the band plan for US is given in figure 2.3 [21].

In Europe, Germany was the first one to announce the release of 800MHz band to mobile services in early 2009 and then in mid 2010 the spectrum was auctioned [20]. Sweden completed its digital switchover in late 2007 and freed up this 800MHz band in 2008 which was later auctioned to mobile companies in early 2011 [20] [22]. Europe follows a CEPT band plan that is based on FDD, as shown in figure 2.3. In Sweden each of the CEPT band is sub-divided in to six sub-bands, FDD1-FDD6, each of 5MHz in size, see figure 2.3 [23].

Table 2.1: Region 1 bands for mobile services

Frequency Band (MHz)	Bandwidth (MHz)
137 – 144	7
146 – 156.5125	10.5125
156.5375 – 156.7625	0.225
156.8375 – 174	17.1625
223 – 328.65	105.65
335.4 – 387	51.6
390 – 399.9	9.9
401 – 406	5
406.1 – 430	23.9
440 – 470	30
862 – 960	98
1350 – 1400	50
1427 – 1535	108
1660.5 – 2690	1029.5
3400 – 4200	800
4400 – 5000	600
5150 – 5350	200
5470 – 5725	255
5850 – 8500	2650
10,000 – 10,450	450
10,500 – 10,680	180
10,700 – 12,500	1800
14,300 – 15,350	1050
18,100 – 19,700	1600
21,200 – 23,600	2400
25,250 – 29,500	4250
31,000 – 31,300	300
31,500 – 31,800	300
36,000 – 47,000	11,000
47,200 – 50,200	3000
50,400 – 52,600	2200
55,780 – 56,900	1120
57,000 – 76,000	19,000
81,000 – 86,000	5000
92,000 – 94,000	2000
94,100 – 100,000	5900

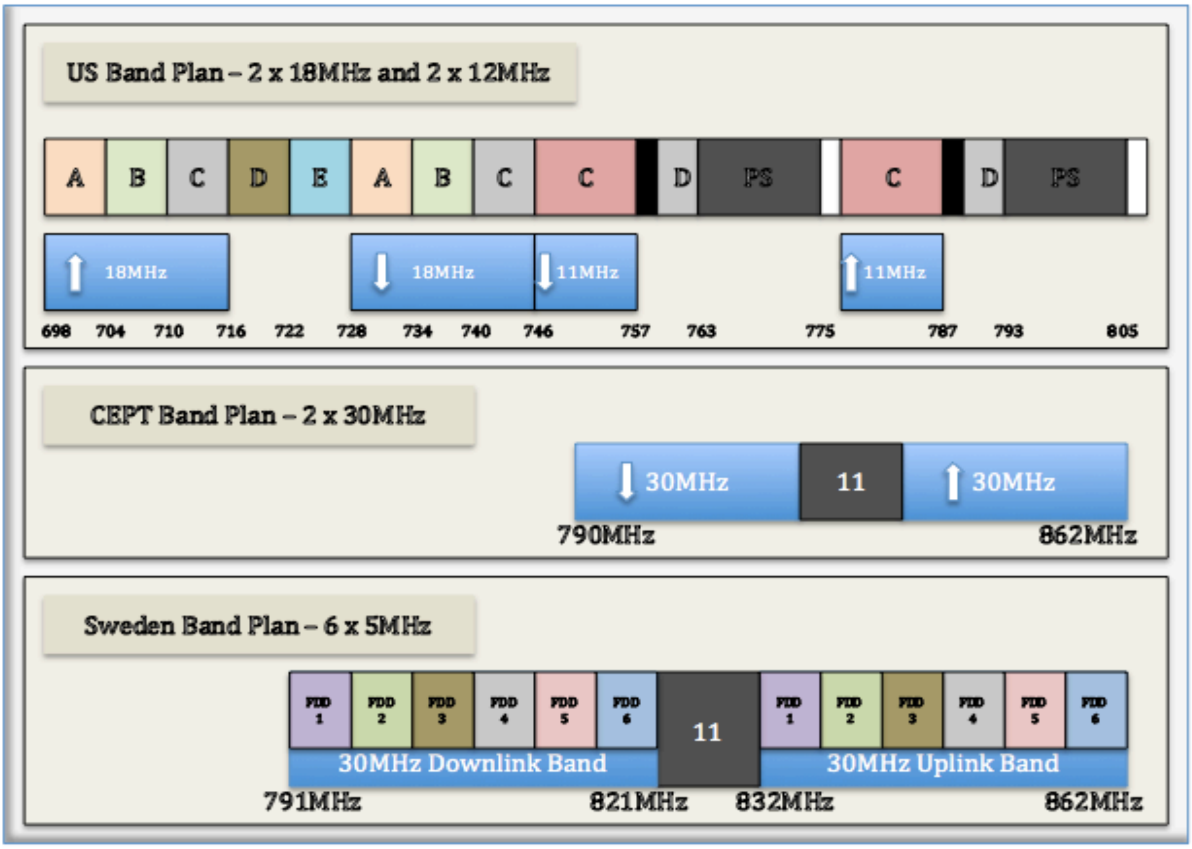

Figure 2.3: The Digital Dividend (DD) bands

2.3 More New Spectrum – TV White Spaces (TVWSs)

Terrestrial TV services do not use the entire spectrum; as some spectrum is used as a guard band to avoid interference. Moreover, not all the assigned spectrum is used for TV services, at a given location, at all times. This unused and unoccupied spectrum, at the given time in a geographical area, called TV White Space, is available for secondary services on non-interfering and non-protected basis with regards to primary services.

FCC, in June 2002, formed a Spectrum Policy Task Force that was assigned to assist the Commission in recommending and evaluating the changes in spectrum policy. In November 2002, Task Force issued its report and specifically recommended to make these White Spaces available. The report also urged to use both the exclusive-right and common spectrum access models. After reviewing the comments on its Notice of Inquiry (NOI) from industry, in 2004, FCC issued a Notice of Proposed Rule-Making (NPRM) that specifies the rules for those TVWSs [24]. All these rules are based on the recommendations received from NOI and provide a basis for FCC Report and Order (R&O), which sets the practical limits for unlicensed devices trying to access those white spaces.

Table 2.2: WSD outdoor parameters

Parameters	Base Station	User Equipment
Data Rate (Mbps)	1 – 10	0.128 – 2
Transmission Bandwidth (MHz)	5 – 8	0.360 – 5
Receiver Noise Figure (dB)	4 – 7	5 – 7
Antenna Gain (dBi)	7 – 8	0 – 14
Maximum Range (m)	10,000	10,000
EIRP (dBm)	Upto 36	Upto 27

In Europe, CEPT conducted a study and issued its findings on TVWS in ECC Report 24 [25]. They have the similar findings and recommendations as of FCC where both FCC and CEPT recommend using Cognitive Radios (CRs) to access the spectrum for mobile services. In January 2011, a CEPT working group SE43 compiled its findings, on technical operational requirements for TVWS, in ECC Report 159 [26].

In report 159, CEPT defined 470-790MHz to be used as TVWS but the availability of the spectrum depends on the locality [26] [27]. Report retains the original 8MHz TV bands to be used for mobile services. In [26] and [27], following three deployment scenarios are defined:

- Indoor wireless access
- Outdoor wireless access
- Machine-to-machine (M-M) connectivity

There are also two different methods defined for power allocation:

- Fixed output power
- Location specific output power

Location specific output power allocation depends on the whole process of spectrum allocation through the use of geo-location databases and then CR determines the suitable transmit power for the white-space device (WSD). While in Fixed output power allocation, some strict limits have already been defined in [26] and [27], as given in table 2.2. These fixed EIRP limits are not only the limits for fixed output power allocation but it also serves as the upper bound for location specific power allocating services.

So, we have seen that originally there is lots of unused spectrum available, especially at the higher frequencies. In the next chapter we would see how these frequencies respond to capacity and coverage demands. Also, in future we could see lot more of those dividend spectrums and white spaces being available for cellular usage.

Chapter 3

RF Link Budget

The performance matrix of a newly deployed communications system depends on how far it can cover and what throughput we can get. Along with many other factors that affect the performance of the system, the most important ones are the permitted transmit power, available bandwidth and receiver system sensitivity. In general, the bandwidth and available signal power at the receiver define the system capacity, as according to Shannon channel capacity

$$C = B\, log_2(1 + |h|^2 S/N). \tag{3.1}$$

In equation (3.1), there are two most important parameters bandwidth B and signal-to-noise ratio S/N. However, in perspective of link budget, the quantity of greatest interest is SNR, since it is the ability of the receiver to detect the correct output from received signal S, impaired due to channel h, in the presence of receiver noise N with an acceptable error probability [28].

The signal S depends on gains and losses of the whole communication system. Link budget lists all those gains and losses that affect the SNR at the receiver. In general all the system gains and losses can be categorized into three groups, for easier understanding

- Transmitter gains and losses
- Channel losses
- Receiver gains and losses

The simplest of the link budget equation found in the literature is known as Friis' transmission equation and is given below

$$P_r = P_t G_t G_r \left(\frac{\lambda}{4\pi d}\right)^2, \tag{3.2}$$

where,

P_t and P_r are transmitted and received powers, respectively
G_t and G_r are transmitted and received antenna gains, respectively
λ is the wavelength of transmitted signal
d is the separation distance between transmitter and receiver

Equation (3.2) is a good estimate of how much is the range of the system, given the powers and gains. But a thorough study of link budget involves all the gains and losses present in transmitter, channel and receiver, as depicted in figure 3.1.

3.1 Transmitter Gains and Losses

The purpose of a transmitter is to process the information in a way that is transferable on a given channel. On the way to this process, there are certain elements that add the gain and some introduce the loss in the system. There are three main components of a transmitter that affect the link budget calculations;

- Transmit power
- Transmitting antenna gain
- Cable/feeder losses

For simplicity, and considering the scope of this work, the antennas both at transmitter and receiver are assumed to be isotropic with no feeder loss.

3.1.1 Transmit Power

Transmit power determines the range of a wireless communication system, as given below;

$$p_d = \left({P_t}/{4\pi d^2}\right). \qquad (3.3)$$

In equation (3.3), the term p_d is the power density and it shows how much is the transmitted power P_t at the distance d, the higher the power at farther distances the more the area will be covered by the transmitter. Apparently, one would want to cover larger distances but it causes problems; higher power systems would interfere with neighboring systems operating at same frequency and also higher radiated power has adverse effects on human health.

So, there are global authorities that define some limits on how much radiation a person can be exposed to in order to not having bad health effects; table 3.1 gives some global limits on power-flux density [29] and [30].

For a typical dense-urban environment, where the cell range is typically small, in the order of few hundred meters, the values for transmit power is quite high from table 3.1, using the equation (3.3). As we said earlier that higher powers will cause interference; so in practice

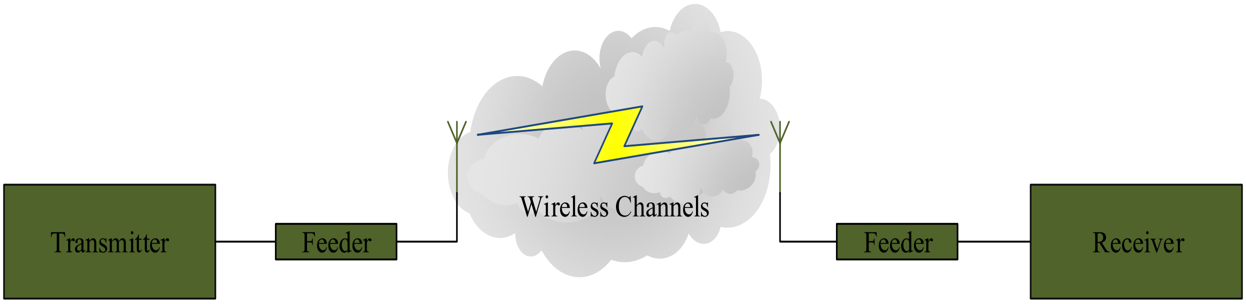

Figure 3.1: A block diagram of a wireless communication system

Table 3.1: Reference limits on transmit power density

Frequency (MHz)	ICNIRP Power Density (W/m^2)	IEEE Power Density (W/m^2)
10 – 400	2	2
400 – 2,000	$f/200$	$f/200$
2,000 – 100,000	10	10

these values are very small, could be several thousand times smaller than these limits.

Based on ITU spurious emission limitation [31], the technology developers like 3GPP and IEEE defines the limits of power to be used in a certain band. Also, the national regulators, like FCC, PTS etc. make sure that the manufacturers fulfill those recommendations before launching their product.

BS and UE are divided into their respective categories to define their power levels. There are four categories defined for UE and their respective power level that lies in the range -40dBm–23dBm, [34][35]. There are also three classes of BS defined by 3GPP, in [32] [33], and there is no upper transmit power limit defined for macro BS. So in the end, for a transmitter, manufacturer sets the maximum transmit power and make sure to conform to ITU spurious emission requirements.

However, PTS puts an upper bound on ERP to be maximum 25W (EIRP≈46dBm), for mobile radio services in bands above 47MHz [18]. Moreover, there have been some other studies in order to get the channel characteristics, one such study by METIS [36], while studying the dense-urban scenario, the 43dbm/10MHz transmit power is used for a macro BS operating at 800MHz.

Additionally, some numbers are collected from the data sheets of different power amplifiers from three different manufacturers. These manufacturers are

- Hittite Microwave Corporation
- United Monolithic Semiconductors (UMS)
- Advanced Semiconductors Business Inc. (ASB)

The output power of a transmitter, in general, is dependent on how much power the power amplifier can generate. There is no proper mathematical equation to show the actual behavior of the transmitted power against frequency but there is a general trend of low power generation at higher frequencies because of the complexity of the hardware used at those frequencies, as can be seen in figure 3.2. The blue and magenta curves are the 3rd order polynomial fits to the mean and standard deviation plots of 1dB compression point output power, respectively. These power levels were taken, mostly, for low and medium GaN power amplifiers. So, to compensate for those lower power levels, higher directivities at higher frequencies would be used to balance out the EIRP levels.

3.2 Channel Losses

A wireless medium between a transmitter and receiver is an open space and it consists of several phenomena that affect the signal propagation. Primarily, the distance between transmitter and receiver is a major factor that influences the received signal. Secondly, the atmosphere and its different factors absorb the signal energy. Then, the objects present in the propagation path of the transmitted signal also affect the transmission. Unlike the transmitter, all the affecting procedures in the channel attenuate the signal.

3.2.1 Path Loss

Path loss is an important measure in the design of a communication system. It determines the range of a communication system for a given acceptable received power level. This determination of range helps to define what transmitted power should be used and what different antenna parameters like antenna gains and their heights etc. could be used.

From equation (3.3), the power density, for a fixed transmit power, reduces as the distance increases. This reduction in power density due to distance is called the free-space path loss. But, in actual, path loss involves many factors affecting the signal, like

- Free-space propagation loss
- Atmospheric phenomenon causing absorption
- Big objects causing shadowing
- Scatterers causing fading

All these factors depend on frequency and some of them also depend on the environment.

There are several models in the literature to calculate the path loss. The simplest and the most common is the free-space path loss model, given below

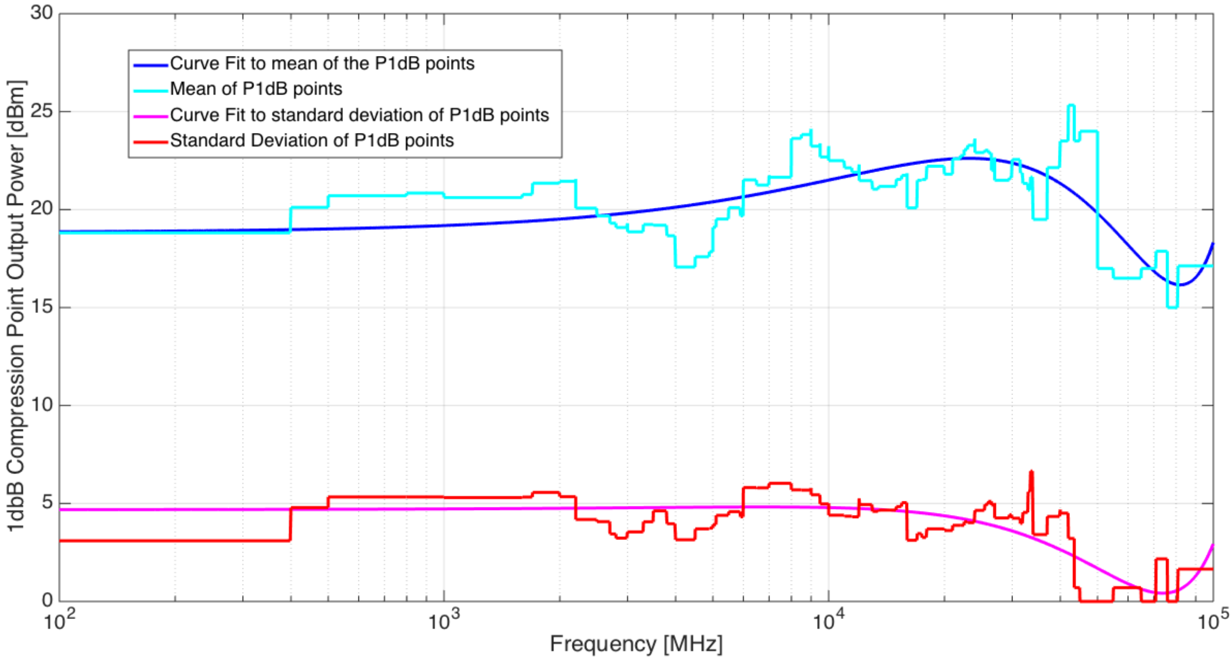

Figure 3.2: Mean and standard deviation for P1dB output power to show the power vs frequency behavior

$$L_s[dB] = 32.4 + 20\,log_{10}\,f_{MHz} + 20\,log_{10}\,d_{km}. \tag{3.4}$$

There are other empirical models discussed in detail in academic literature [37][38]

- Okumura Model
- Hata Model
- COST-231 model

Unlike the free-space model, which can be used only for a generic LoS path in any scenario, these models are scenario dependent and also depend on other parameters. These scenarios could either be urban or sub-urban, so with relevance to the scope of this work only dense urban scenario is considered.

Apart from the literature there are several other path loss models that are being studied and developed. Different working groups have previously defined models that were deployed for former-generation of communication systems. Also, some groups are working on new models to be deployed for 5G. Some of the previous models are listed below

- ITU UMa model [39]
- 3GPP macrocell path loss model [40]
- WINNER urban macrocell model [41]
- METIS dense urban model [36]

All of these models are very much frequency and distance dependent and are valid for a certain range of frequency and other parameters, except of free-space model. So, for the simulation purposes, the simplified log-distance path loss model is used for the frequency ranges outside of the above mentioned models, which is given by [37][38]

$$\overline{PL}(dB) = PL(d_o) + 10n \log_{10}\left({}^{d}/_{d_o}\right). \qquad (3.5)$$

The two model parameters, n the path-loss exponent and d_o the reference distance are chosen on the basis of studies conducted in [42] and [43]. In our case, n and d_o are chosen for an urban scenario and set to be 6 and 20, respectively.

All these models are used for dense urban scenario and certain assumptions have been made in this regard. In general, BS and UE antenna heights are taken 25 and 1.5 meters, respectively. The average building height and street width is considered to be 20m each, while the spacing between the far edges of buildings is 95 meters.

All these models are studied to check their relative behavior and, as can be seen in figure 3.3 that, these models closely follow each other, except free-space and log-distance models. Free-space model represents a LoS condition, so it gives best possible conditions for path losses. In log-distance model, parameter path loss exponent is far greater than those used in other empirical models, so it gives the losses in worst-case scenario. All the other empirical models closely follow each other, since the parameters are almost similar. Also, working empirical models are derived from basic empirical models, like 3GPP model is based on COST-231 model. It is to clear, in figure, COST-231, 3GPP and WINNER models almost overlap each other. All these models, except free-space model, are for non-LoS dense urban macrocell scenario.

Figure 3.4 shows the path loss in 3D with both the frequency and distance as variable. The two other subplots show the xz-plane and yz-plane, respectively. The WINNER model is used for these plots. This figure shows how the path loss varies when either both or one variable changes with relative to each other. This figure also shows that distance is the dominant factor in path loss, as the slope is greater in path loss vs. distance plots than that of path loss vs. frequency plots.

In MATLAB, three models are used, Hata (150-450MHz), WINNER (450-6000MHz) and log-distance (6-100GHz).

3.2.2 Atmospheric Losses

The cellular systems operate in the tropospheric region of the earth that is the main constituent of losses in the atmosphere. Our atmosphere consists of several phenomenon that affect the transmission but in the cellular frequency range there are three main constituents that absorb the signal energy [44] [45] and [46]:

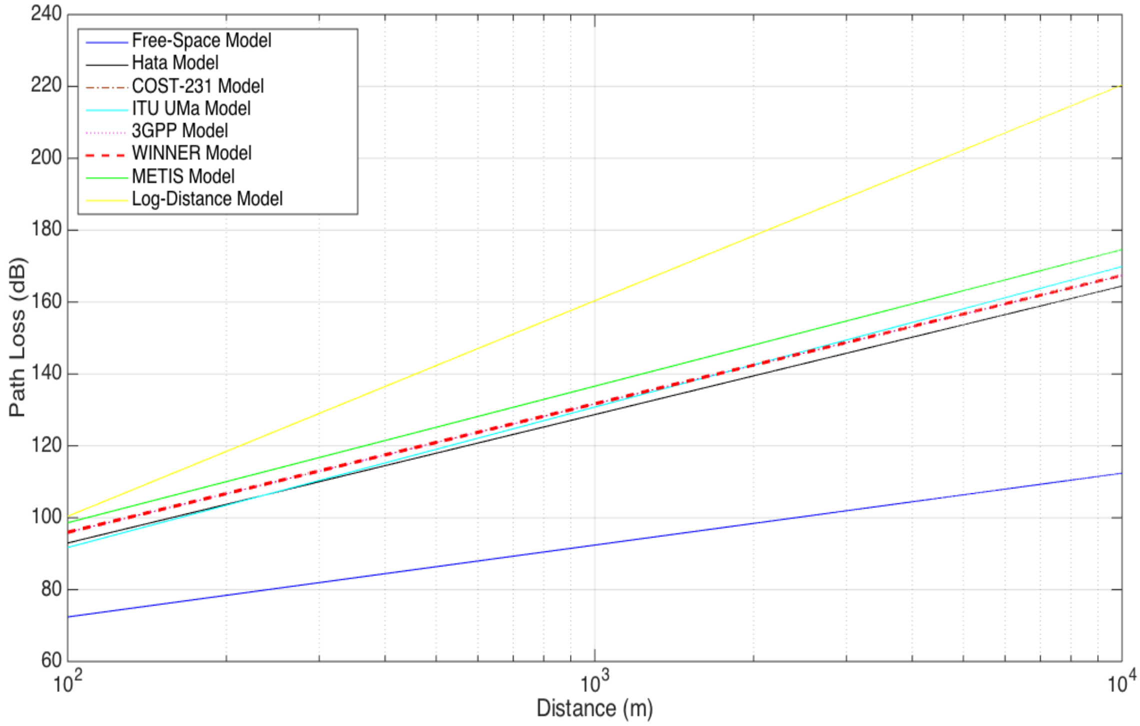

Figure 3.3: Different path loss models - Path Loss vs Distance for fixed carrier frequency fc = 1GHz

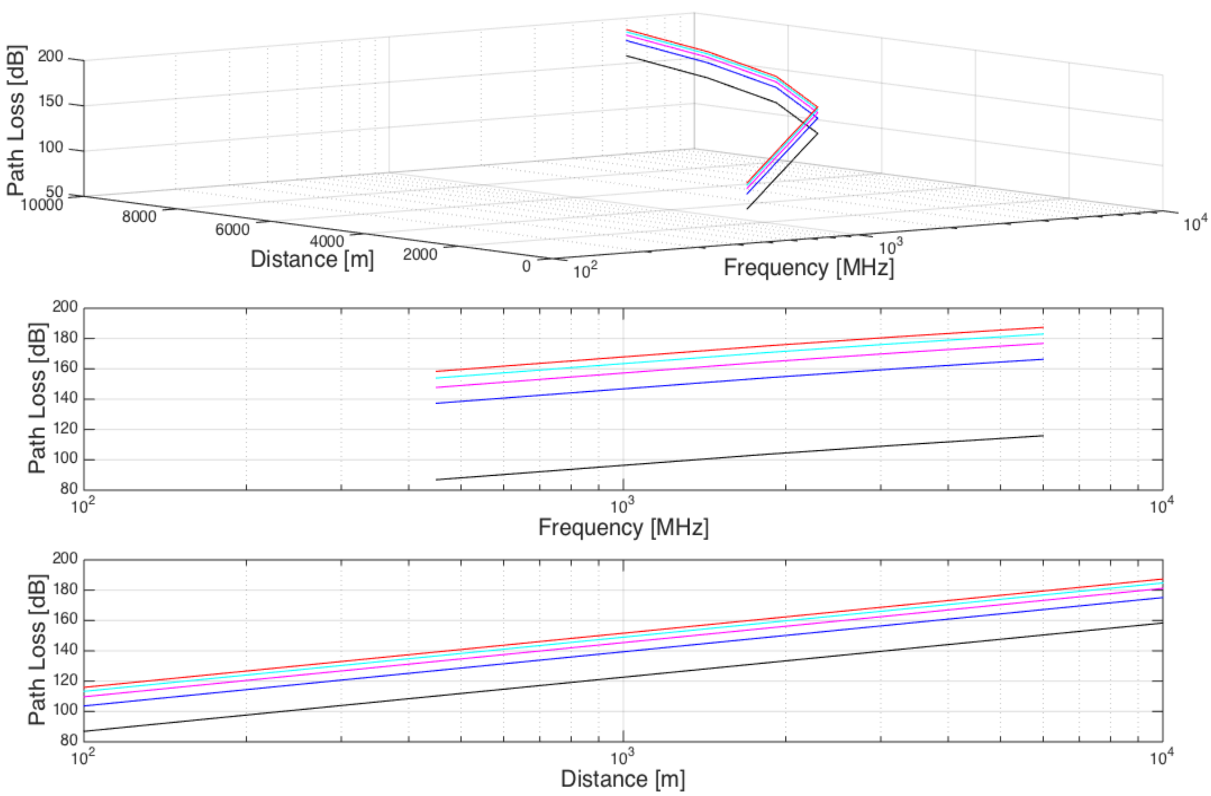

Figure 3.4: 3D WINNER model path loss with f [MHz] vs. PL[dB] in xz-plane and d[m] vs. PL[dB] in yz-plane

- Gaseous absorption due to O_2 and H_2O molecules
- Attenuation due to rain
- Attenuation due to fog

All of these losses depend on frequency and their respective constituents but, for a given frequency, they increase as the signal travels long through the medium. Also, these losses are negligible for frequencies below 10GHz, as can be seen from the curves of these three losses in figures 3.5, 3.6 and 3.7 respectively.

All these curves depend on the specifications of environment; so, different parameters are required to study them. For gaseous losses standard parameters are chosen; while, for rain attenuation rain rate is set to $60\,mm/hr$ with vertical polarization and for fog attenuation liquid density in fog is set to $0.15\,g/m^3$.

3.2.3 Shadowing

Empirical path loss models do not account for surroundings of the receiver. For a same distance, at different locations in a cell, surroundings might be different. Thus, the received power would be random about the mean signal strength given by the median path loss. This random phenomenon of variable received power is due to the shadowing. So, the total path loss can be expressed as

$$L_t[dB] = L_s[dB] + X_{\sigma_{dB}}[dB]. \tag{3.6}$$

In equation (3.6), $X_{\sigma_{dB}}[dB] \sim \mathcal{N}(0, \sigma_{dB}^2)$ is the shadowing factor and is modeled as a log-normally distributed random variable [37]. There have been empirical studies to determine the value of σ_{dB}^2 and it is shown that it varies in the range 5–12 in a macrocell [47]–[53].

There have been some studies on measuring the path loss and shadowing variations in different bands and locations, mentioned in [54]. These studies show that the shadowing is mainly location dependent, instead of frequency. In [55], three measurements were taken for path loss, two in Aarhus, Denmark and one in Stockholm, Sweden for a system operating at 1.8GHz. The standard deviation for shadowing was found 7.9dB and 7.3dB at Aarhus for 20 and 32 meters antenna heights and for an antenna height of 21 meters at Stockholm the standard deviation was recorded to be 8.5dB.

In another study in Tokyo, Japan, path loss measurements have been conducted at 457.2MHz, 813MHz, 2.2GHz, 4.7GHz, 8.45GHz and 15.45GHz both in macrocell and microcell [56]. The results for macrocell, at a distance greater than 1km, are shown in table 3.2.

There are some other studies too that show the shadowing dependence on frequency as well, [56]. There is one empirical model, given in [48], which is valid for a range up to 20GHz [57]. The model is given below

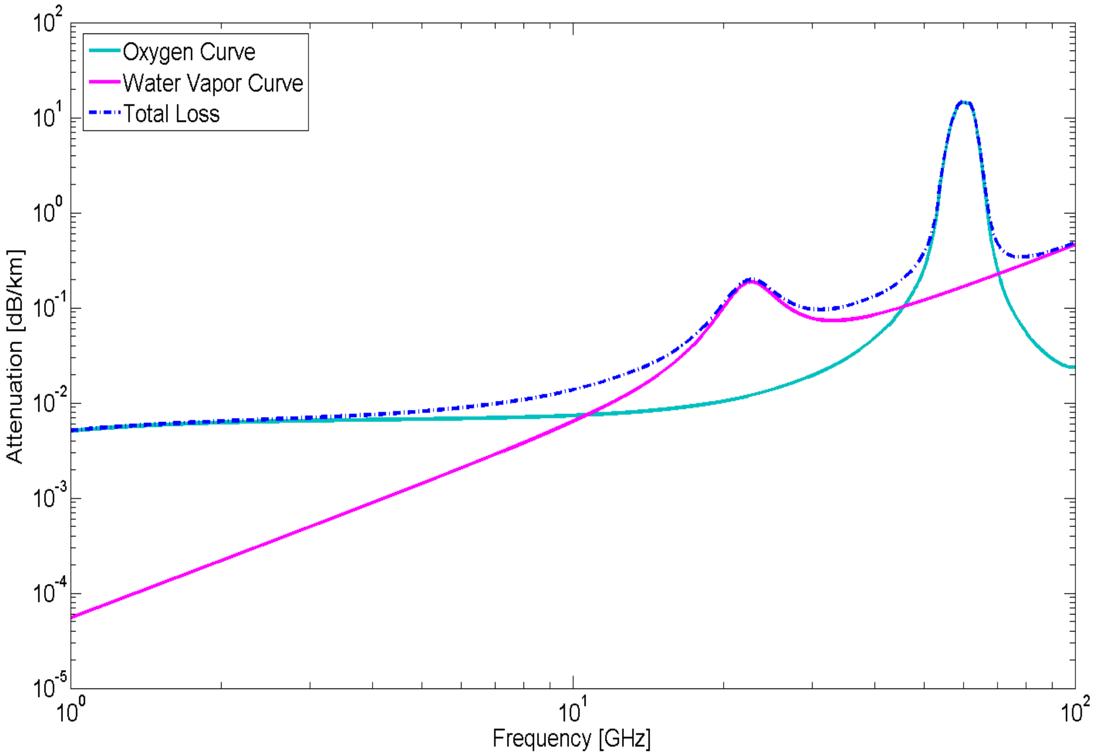

Figure 3.5: Gaseous losses in [dB/km] for standard atmosphere parameters

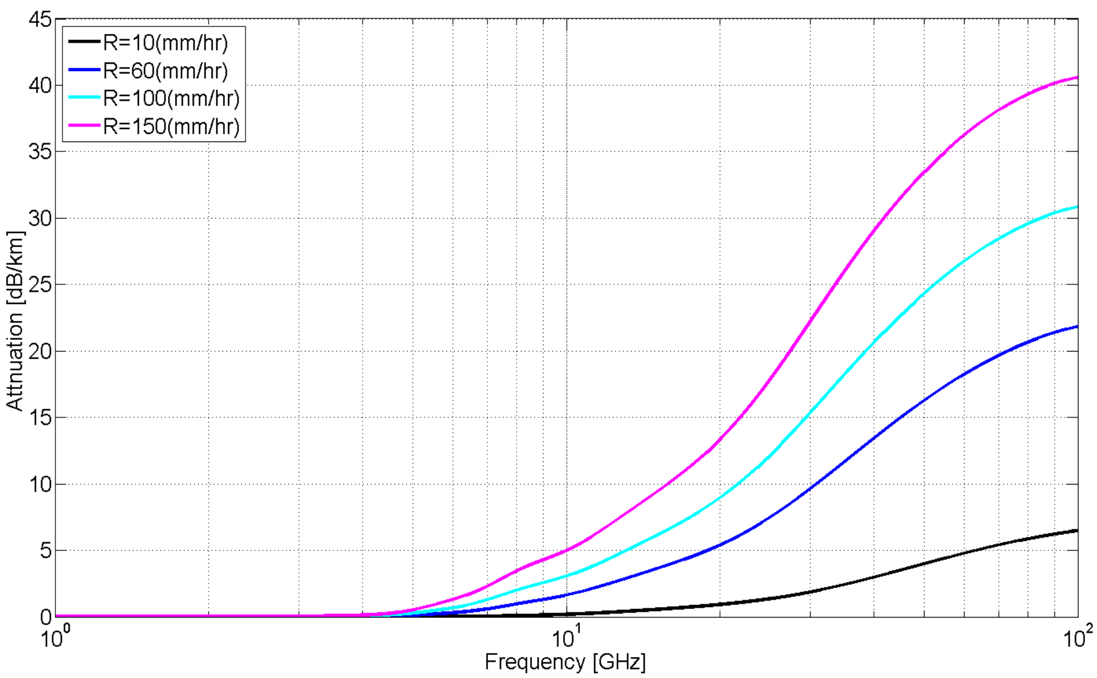

Figure 3.6: Rain losses in [dB/km] for different rain rates

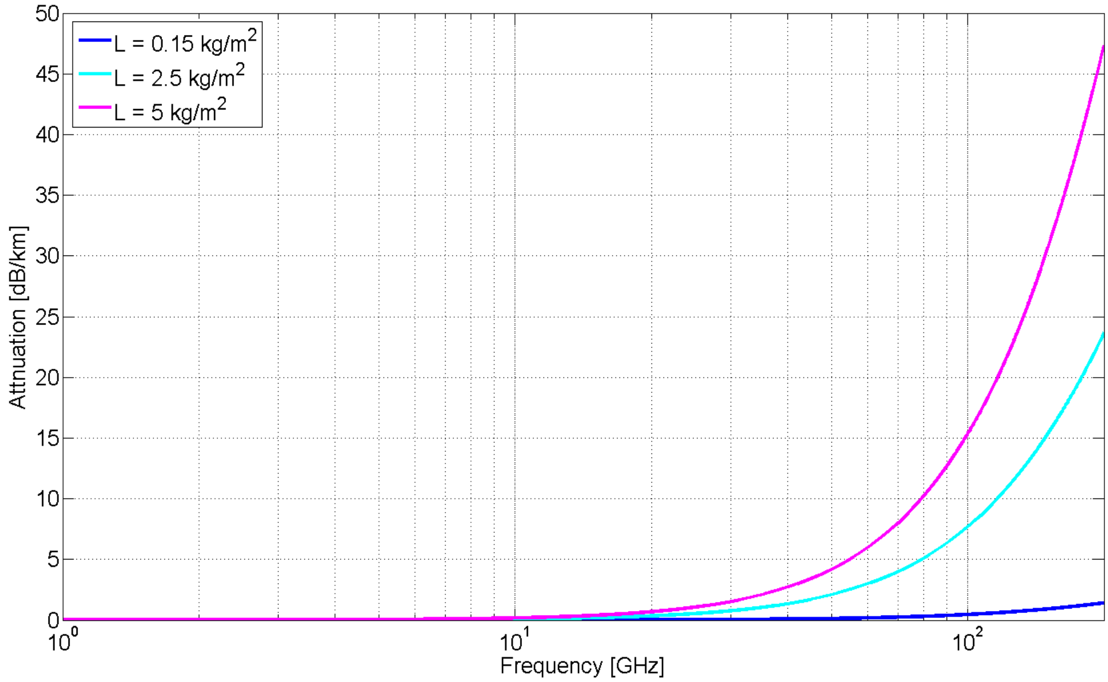

Figure 3.7: Fog losses in [dB/km] for different water densities in atmosphere

Table 3.2: Standard deviation for shadowing

Area	457.2MHz	813MHz	2.2GHz	4.7GHz	8.45GHz	15.45GHz
Nakano	7.47		7.61	7.67		7.25
Ikebukuro	5.30		5.52		6.17	6.08
Honjo	4.85	7.37	6.58		6.32	4.32
Nippori	5.36		6.35		5.95	6.58

$$\sigma_{dB} = 0.65(log_{10} f_{MHz})^2 - 1.3\, log_{10} f_{MHz} + A. \qquad (3.7)$$

Here, A is 5.2 in urban and 6.6 in suburban environment. For doubling the frequency, in urban scenario, the standard deviation increases by 1dB.

So, looking at both the measurement studies and the empirical model, it can be safely assumed that the model is not a valid fit to shadowing in real-time scenarios, as it does not take into consideration the surrounding environment. Shadowing is a very important parameter as it helps in determining the margin for the communication system, so proper consideration needs to be done when considering the values for it.

3.2.4 Multipath Fading

Multipath fading is another limiting factor in a cellular communication system [37]. In dense urban scenarios fading occurs due to reflections of the scattered paths, even if there is a LoS path available. The incoming waves, from different directions, have randomly distributed amplitude and phases. These signals could either have constructive or destructive effect while adding [38]. The destructive addition, when phase do not match, cause deep fades and this limits the transmission performance.

The received power is random due to multipath effect, giving rise to random SNR at the receiver. The envelope of the received signal is Rayleigh distributed but the SNR is modeled having an exponential distribution, given below

$$p_{\gamma}(\gamma) = {}^{1}/_{\bar{\gamma}}\; exp\left(-{}^{\gamma^2}/_{\bar{\gamma}}\right) \qquad (0 \leq \gamma \leq \infty), \tag{3.8}$$

where, γ is instantaneous SNR and $\bar{\gamma}$ is average SNR.

This randomness of the channel causes deep fades and data is lost, an important figure of merit to measure the fade is outage probability that determines on how much marginal power needs to be transmitted [37].

3.3 Receiver Gains and Losses

Receiver system undoes all the processing done by the transmitter on the original information but the important metric for receiver is the SNR value. If the coming signal does not have the strength over a certain threshold then receiver cannot process that signal. Both the receiving antenna and receiver system adds to the SNR, in terms of gain and noise.

Each component in the receiver has certain gain that affects the overall receiver noise floor, important figure-of-merit, called receiver sensitivity.

3.3.1 Receiver Sensitivity

Receiver consists of the electronic circuitry, which due to inherent properties, induce thermal noise in the receiver. The noise power related to that temperature is called the receiver sensitivity. As it is said earlier that this sensitivity defines the noise floor of the receiver, so for a good recovery of the transmitted signal the received signal power must need to be higher than the sensitivity. The receiver sensitivity of a receiver for a given bandwidth can be written as

$$N = kT_{sys}B, \tag{3.9}$$

and

$$T_{sys} = T_A + T_{comp}, \tag{3.10}$$

where,

k is Boltzmann's constant
T_{sys} is effective noise temperature of receiver system
B is receiver bandwidth
T_A is noise temperature of antenna
T_{comp} is composite receiver noise temperature

The receiver noise temperature is an important performance metric of the receiver and it depends on the noise figure of the receiver, as given below [28]

$$T_{comp} = \left(F_{comp} - 1\right)T_o, \quad (3.11)$$

where,

F_{comp} is the composite noise figure of the receiver components
$T_o = 290K$ is the reference temperature

The total noise figure, in a system, depends on the gains of the individual components, as given below

$$F'_{comp} = F_1 + \frac{F_2-1}{G_1} + \frac{F_3-1}{G_1G_2} + \ \dots + \frac{F_n-1}{G_1G_2 \dots G_{n-1}}. \quad (3.12)$$

The noise figure, from the expression above, does not depend on the frequency but it does on the material and the complexity of the individual component and its corresponding gain. Also, the composite value is dominated by the first component, so practically a high gain LNA is used to keep that value to minimal. Figure 3.8 shows a generic trend for noise figure, the values are taken from data sheets of different LNAs from different manufacturers. These manufacturers are:

- BnZ Technologies
- M/A-COM Technology Solutions Holdings, Inc. ($MACOM_{TM}$)
- Hittite Microwave Corporation
- Advanced Semiconductors Business Inc. (ASB)
- United Monolithic Semiconductors (UMS)
- Low Noise Factory
- HXI, LLC
- TriQuint

Similarly, the antenna also adds the noise to the signal but this noise it receives from the environment, represented as

$$T_A = \frac{1}{4\pi}\int_0^{2\pi}\int_0^{\pi} G(\theta, \emptyset)T_b(\theta, \emptyset) \sin\theta \ d\theta d\emptyset. \quad (3.13)$$

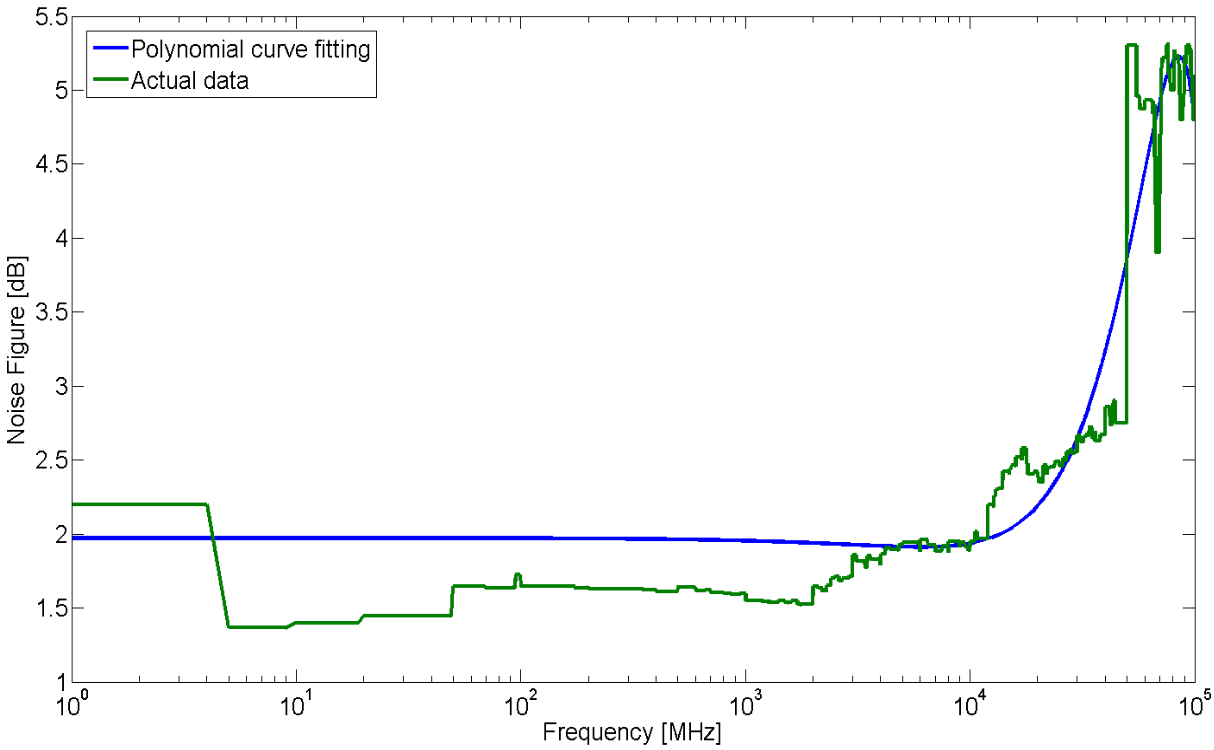

Figure 3.8: Noise figure values for different LNAs from different manufacturers and a curve fit to that data

As it can be seen that the antenna temperature depends on the pointing angle of the main beam and the corresponding received brightness temperature T_b in that cone angle. It is very hard to find suitable expression for cellular system but still there are some calculations given in academic literature for satellite systems. So, for simplicity a reference temperature of 290K is assumed for our calculations.

3.4 Cell Coverage Area

Cell coverage area is sum of all the fractional-areas, which are not in the outage due to shadowing or deep fade event, it is represented in percentage. Since the deep-fade could be temporary but a shadowed region could exist permanently in some spot in a cell, either close to the cell or somewhere far away. So, the coverage area is calculated under the shadowing alone [37].

From figure 3.9, consider a mobile user anywhere in the cell at a distance r having a probability that it is not in outage [37][38].

$$Pr(P_r(R) \geq P_{min}) = 1 - P_{out} = Q\left(\left(P_{min} - \overline{P_r}(R)\right)\Big/\sigma_{dB}\right). \qquad (3.14)$$

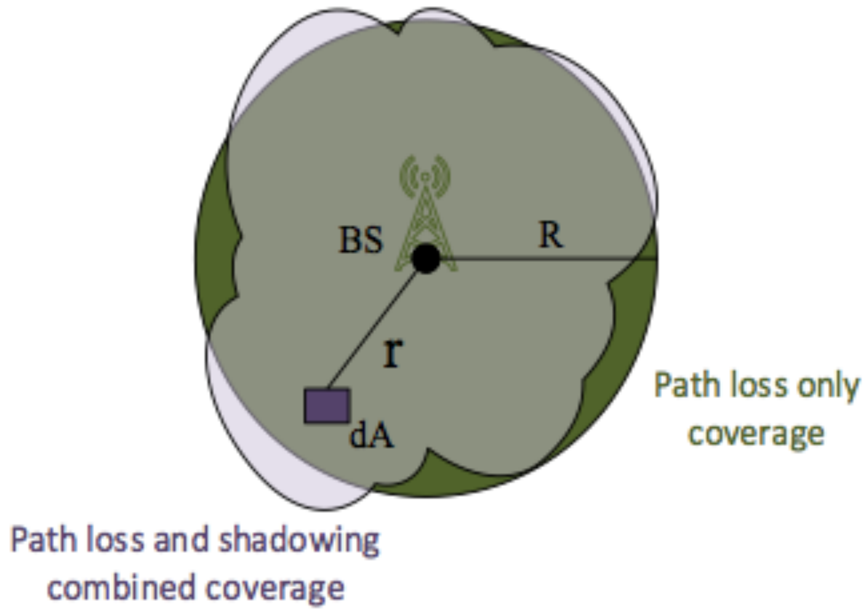

Figure 3.9: Cell coverage area

So, by definition

$$Coverage = {}^{1}\!/_{\pi R^2} \int_0^{2\pi} \int_0^R Pr(P_r(r) \geq P_{min}) r \, dr \, d\theta. \quad (3.15)$$

From equation 3.14

$$Pr(P_r(r) \geq P_{min}) = Q\left(\frac{P_{min} - \left[P_t - \left(\overline{PL}(d_o) + 10n \log\left({}^{r}\!/_{d_o}\right)\right)\right]}{\sigma_{dB}}\right). \quad (3.16)$$

But the path loss at the cell boundary, $(r = R)$

$$\overline{PL}(r) = \overline{PL}(d_o) + 10n \log\left({}^{R}\!/_{d_o}\right) + 10n \log\left({}^{r}\!/_{R}\right). \quad (3.17)$$

Now using equation (3.17) in (3.14)

$$Pr(P_r(r) \geq P_{min}) = Q\left(\frac{P_{min} - \left[P_t - \left(\overline{PL}(d_o) + 10n \log\left({}^{R}\!/_{d_o}\right) + 10n \log\left({}^{r}\!/_{R}\right)\right)\right]}{\sigma_{dB}}\right). \quad (3.18)$$

Let, $a = \left\{ \left(P_{min} - \left[P_t - \left(\overline{PL}(d_o) + 10n \log\left({}^{R}\!/_{d_o}\right)\right)\right]\right) \Big/ \sigma_{dB} \right\}$,

and $b = \left({}^{n}\!/_{\sigma_{dB}}\right) 10 \log e.$

Using a, b and equation (3.18) in equation (3.15) becomes

$$Coverage = \frac{2}{R^2}\int_0^R rQ(a + b\ln(r/R))dr. \tag{3.19}$$

The equation (3.19) can be expressed in a closed-form solution,

$$Coverage = Q(a) + exp\left(\frac{2-2ab}{b^2}\right)Q\left(\frac{2-ab}{b}\right). \tag{3.20}$$

From above expression, we get that coverage area mainly depends on path loss exponent, shadowing and threshold power. For P_{min}, reference signal received power (RSRP) from 3GPP TS 36.214 is chosen as a suitable parameter. RSRP is defined as the average power of the resource elements that carry cell-specific reference signal (CSR), over operating bandwidth. According to TS 36.133, the reporting range of RSRP is -140dBm to -44dBm. So, considering a worst-case scenario, P_{min} is set at lowest of RSRP i.e. -140dBm.

3.5 Shadow-Fading Capacity

An AWGN channel is modeled as

$$y = x + N, \tag{3.21}$$

where x is the signal transmitted over the AWGN channel, y is the channel output and N is the white zero mean noise.

The capacity of such a channel is given in equation (3.1), which is an upper bound. But the radio channel has total random characteristics due to three main phenomena in the channel; those are reflections, diffraction and scattering. These three phenomena along with distance result in attenuation, large-scale shadowing and small-scale fading. The attenuation is due to the separation distance between BS and mobile user and shadowing is caused due to multiple reflections and/or diffractions [60]. Multipath scattering causes the small-scale fading, which can cause significant variation in received power or a deep fade [60]. The small-scale flat fading is modeled as shown in figure 3.10 and expressed by [60]

$$y = \sqrt{A}e^{j\varphi}x + N, \tag{3.22}$$

In equation (3.22), the term $\sqrt{A}e^{j\varphi}$ is the complex channel gain with amplitude $\sqrt{A}$ and phase φ. The phase is uniformly distributed and in $[0,2\pi)$ while A is a random variable with Rayleigh fading distribution. Now the instantaneous SNR would be

$$\gamma = A\left(S/_N\right). \tag{3.23}$$

Using the Shannon ergodic capacity, given that CSI is known only at receiver [37]

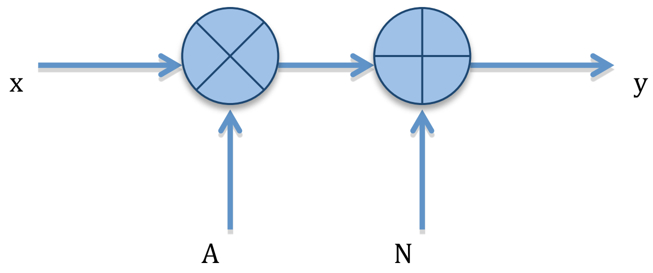

Figure 3.10: System model of a fading channel

$$C = \int_0^\infty B \log_2(1+\gamma)p(\gamma)d\gamma. \tag{3.24}$$

As mentioned in section 3.2.4 that SNR is exponentially distributed in Rayleigh fading channel but shadowing is also present in the channel. So, the channel acts as a composite of Rayleigh-lognormal channel. There have been some studies, both in literature and research [61] [62] and [63], to model the composite SNR with different distributions but a simple Rayleigh-lognormal distribution is given by

$$p_\gamma(\gamma) = \int_0^\infty p_{\gamma|\gamma_o}(\gamma|\gamma_o = \overline{\gamma_o})p_{\gamma_o}(\gamma_o)d\gamma, \tag{3.25}$$

$$p_{\gamma|\gamma_o}(\gamma|\gamma_o = \overline{\gamma_o}) = {}^1\!/_{\gamma_o}\ \exp\left(-\gamma/\gamma_o\right), \tag{3.26}$$

and

$$p_{\gamma_o}(\gamma_o) = \frac{A_o}{\sqrt{2\pi\sigma_{dB}^2\gamma_o}} exp\left(-{}^{(10\log N\gamma_o - \mu_{dB})^2}\!/_{2\sigma_{dB}^2}\right). \tag{3.27}$$

The final expression for equation (3.25) is quite complex to compute. So, to calculate the capacity a random vector is generated for shadowing, for a given standard deviation, and capacity is averaged over that whole vector. There was one expression found in [62] but it is not used here due to not having any proof of reliability of that expression.

Chapter 4

Spectrum Efficiency

As described in chapter 2 that IMT/LTE-Advanced have improvements in lots of sections, more importantly the user throughput and cell and user spectral efficiency. From the Shannon channel capacity theorem, for a fading channel h, the throughput is

$$R \leq C = B \log_2(1 + |h|^2 SNR) \qquad (bps), \tag{4.1}$$

and the cell and user spectral efficiencies can be represented by followings [64], respectively

$$\eta_{cell} = \textstyle\sum_i^N \chi_i / T.B.M \qquad (bps/Hz/cell), \tag{4.2}$$

and

$$\eta_{user} = \chi_i / T.B \qquad (bps/Hz), \tag{4.3}$$

where χ_i is the number of correctly received bits for user i in a system with N users and M cells and B is the channel bandwidth while T is the user transmission time.

From above equations (4.1)-(4.3), it can be seen that the most important parameter that affects both the user throughput and two efficiencies is the bandwidth. Since, the throughput is linearly proportional to bandwidth, so if the user has sufficiently large bandwidth available then it can meet the advanced requirements. But, as can be seen from table 3.1, very small chunks are available at lower frequencies that are currently being used for macro-cellular services, as compared to higher frequencies. Moving all the systems to those higher frequencies is not feasible mainly due to cost including new systems being deployed and need for more BSs.

So, moving to higher frequencies for higher bandwidth availability is not the solution alone. There are some means defined to improve spectral efficiencies in 5G systems. Also, a new way is defined to access the higher bandwidth while still operating into lower cellular bands. So, following solutions are being considered for performance enhancement of the systems beyond 4G (B4G) [65]-[67]:

- Carrier Aggregation (CA)
- MIMO
- Heterogeneous Networks
- Relays
- Coordinated Multipoint (CoMP) Transmission

First three solutions are intended to increase the throughput and the spectral efficiencies, as shown in figure 4.1, while CoMP and Relays are intended to improve the coverage quality. In following sections we will discuss about these techniques and their performance enhancement capabilities.

4.1 Carrier Aggregation (CA)

ITU, in [68] with regards to IMT-Advanced requirements, allows the use of scalable bandwidth up to 100MHz, through single or multiple RF carriers. This process of aggregation of multiple carriers to provide larger scalable-bandwidth is called carrier aggregation [74]. Through extended bandwidth, the peak data rates are increased while it can also improve cell spectral efficiency through the use of scheduling in frequency domain [69][73]. Based on the availability of the spectrum, CA is divided into three categories:

- Intra-band contiguous CA
- Intra-band non-contiguous CA
- Inter-band non-contiguous CA

In intra-band CA, there could be continuous or discontinuous carriers available; the aggregation of continuous carriers is called intra-band contiguous CA while the aggregation of discontinuous carriers is called intra-band non-contiguous CA. In inter-band non-contiguous CA, aggregated carriers are located in different bands located in different parts of the spectrum, as shown in figure 4.2. The carrier is referred to as a component carrier in CA-terminology.

It is worth mentioning here that aggregation of bandwidth is not a new concept, it has been used in 3G systems, like 1xEV-DO REV B and HSPA Evolution [75]. But the form of aggregation was limited to intra-band contiguous. The complexity of the system increases from intra-band contiguous to non-contiguous with inter-band non-contiguous the most complex. But the inter-band CA provides better spectrum utilization [70].

Based on what carriers are there for aggregation, different scenarios could be deployed to take advantage of CA. Four different scenarios are shown in figure 4.3, with two cells with carrier frequencies f_1 and f_2 [71][73][75][76].

In scenario 1, two cells are collocated with f_1 and f_2 from same band and having same beam-directions and patterns. This would be the case of one of the intra-band CA and higher throughputs are achieved by aggregating two available carriers.

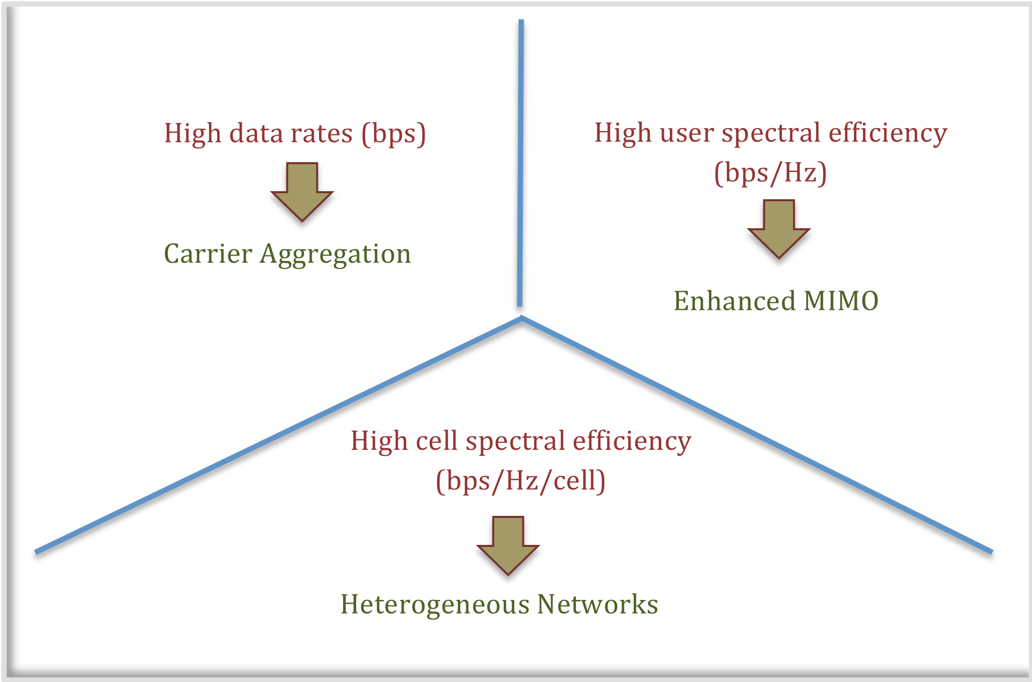

Figure 4.1: Dimensions for performance enhancement in IMT/LTE-Advanced

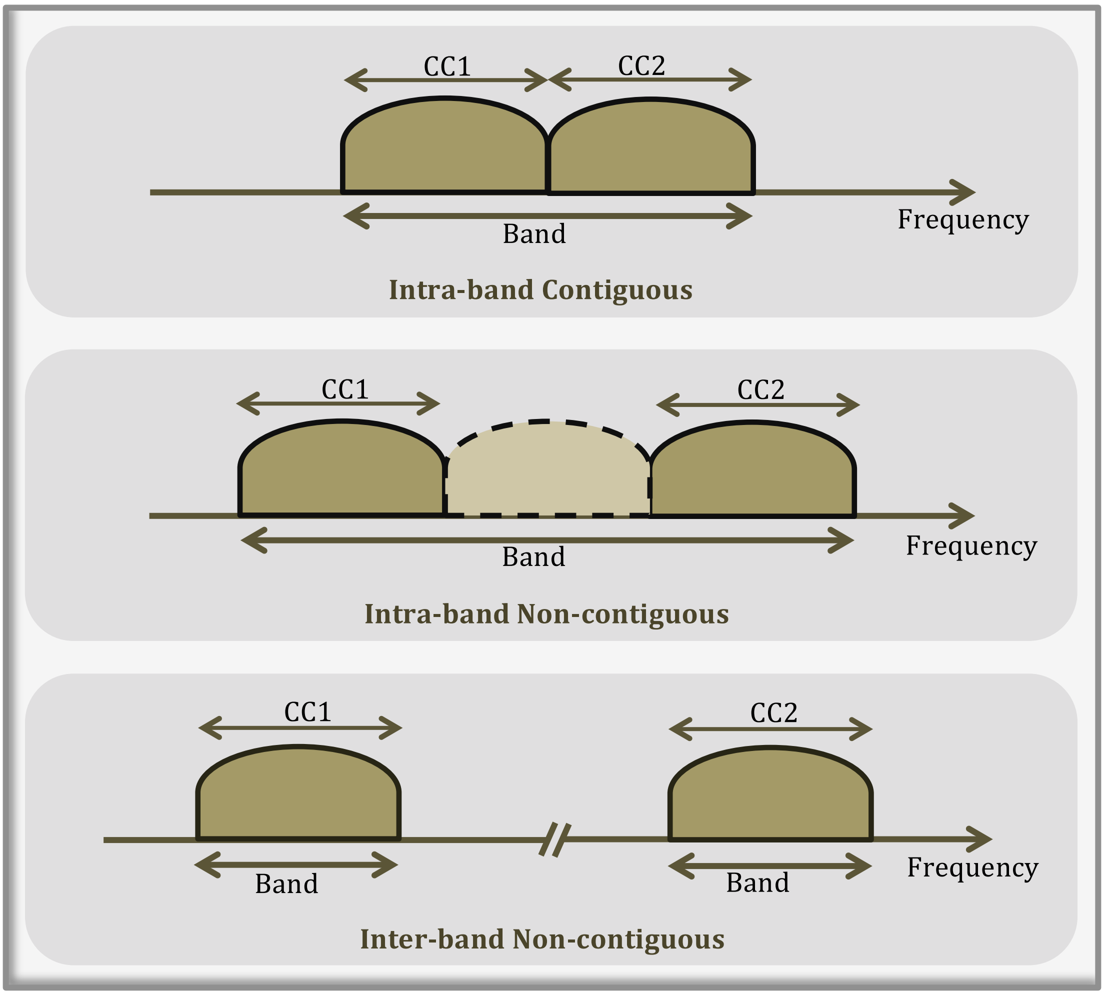

Figure 4.2: Types of CA based on availability of component carrier (CC)

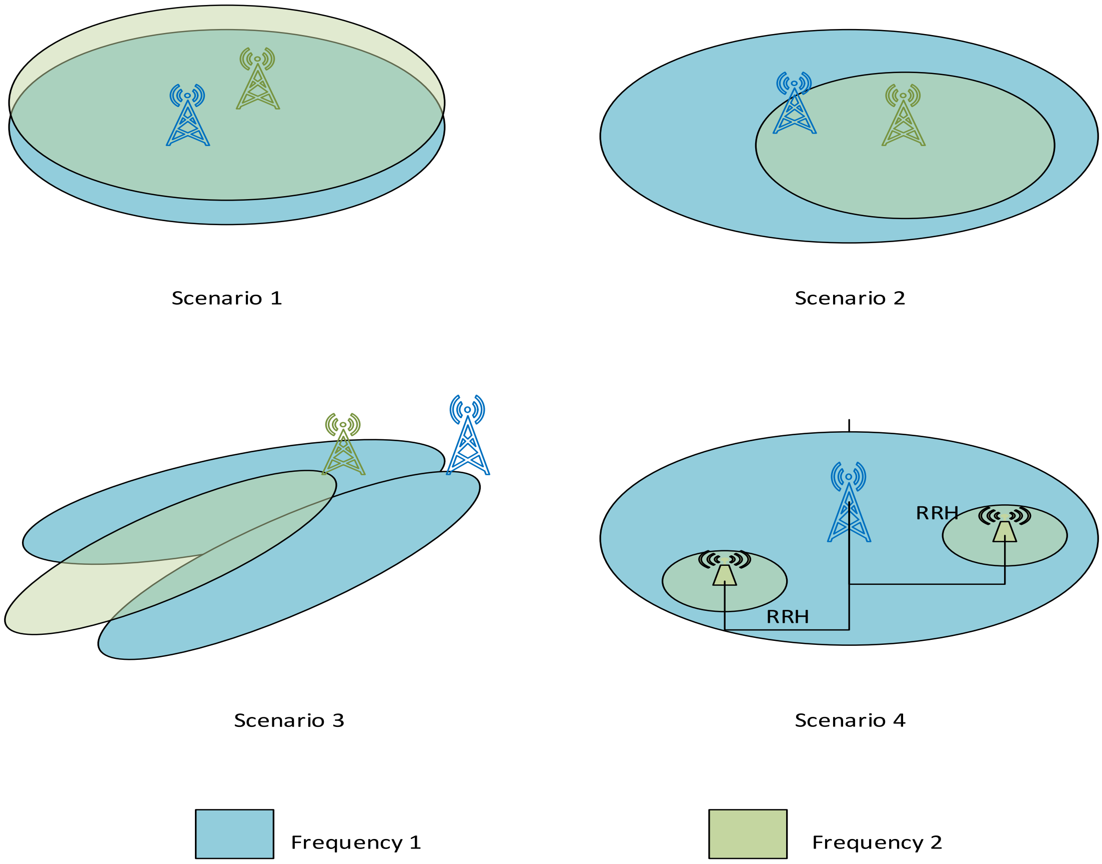

Figure 4.3: CA deployment scenarios

In scenario 2, two cells are collocated and overlaid but f_1 and f_2 are from different bands; thus, two cells have different footprints. The lower frequency BS provides service connectivity while the higher frequency could be used to provide higher throughput to CA-users.

In scenario 3, with any given frequencies f_1 and f_2, two cells are collocated but the beams of second cells are pointed in the direction of sector edges of first cell to improve the cell edge throughput.

In scenario 4, a macrocell provides the basic coverage with, typically lower, carrier f_1 while the remote radio head (RRH) with f_2, from different higher band, provides higher throughput at traffic hotspots. RRH are connected to macro-BS through optical fiber.

From the deployment scenarios it can be seen that not only we can use CA to improve the throughput in the cell but it can also be used to do load balancing and improve cell-edge throughput, S2 and S3 respectively. Pool sharing of the resources allows maximizing the achievable capacity by balancing the load on different carriers based on the user requirements. Also, the availability of the multiple resources to a user increases its average data rate, linearly, in a less loaded network. Moreover, in a loaded network the performance is still better for CA than the non-CA system, while the cell-edge performance reduces to non-CA system. This is illustrated in figures 4.4 and 4.5 respectively, these figures are taken from [73]; more performance results can be seen in [77][78]. Thus, it can be seen that the user throughput is increased, approximately, linearly with aggregated bandwidth.

4.2 Multiple Input Multiple Output (MIMO)

Multiple antenna configurations, both at transmitter and receiver, improve the performance of the system without requiring more power and bandwidth. It is a technique that exploits the spatial-domain in order to improve either the SNR or bandwidth utilization.

The increase in SNR is achieved by the followings:

- Spatial diversity against fading
- Beam-forming

Spatial diversity (SD) is created by transmitting the same data stream over multiple, largely distanced, antennas. Thus, the uncorrelated channel streams experience the different fading characteristics. Now, the receiver has multiple copies of the same data with lesser probability of all the copies being affected by deep fade, figure 4.6, as compared to SISO channel. By effectively combining all those copies, the received signal strength is increased. This increase in SNR is referred to as diversity gain, as following [79]

$$SD\ gain\ (d) = N_T \times N_R, \tag{4.4}$$

where, N_T and N_R are number of antennas at transmitter and receiver respectively.

Beam-forming is a classical array signal processing technique where the transmitter directs its power in the direction of the receiver, given that it has the Channel State Information (CSI) [64][80]. The beam-forming is performed by applying different phase shifts to the transmitted signal, to steer it in the desired direction, as shown in figure 4.7. This concentrated and directed beam provides significant array gain, increasing the SNR by the factor N_T [64][80].

This multiple antenna configuration is also used to create multiple parallel communication channels that provide the higher bandwidth utilization, called spatial multiplexing (SM). In SM, unlike SD, different data streams are transmitted over multiple antennas, as shown in figure 4.8. Thus, without increasing the bandwidth, higher throughput is achieved. This increase in throughput is called spatial multiplexing gain, given below

$$SM\ gain\ (r) = min(N_T, N_R). \tag{4.5}$$

Since, there are r numbers of parallel channels created; so, from equation (4.1), capacity is

$$C_{SM} = r \times \left(B\ log_2\left(1 + |h|^2 \frac{S \times N_R / r}{N}\right)\right). \tag{4.6}$$

The highest capacity is achieved if the radio conditions are good, implying higher SNR. From above expression, it can be seen that the capacity could be increased linearly if N_t and N_R are

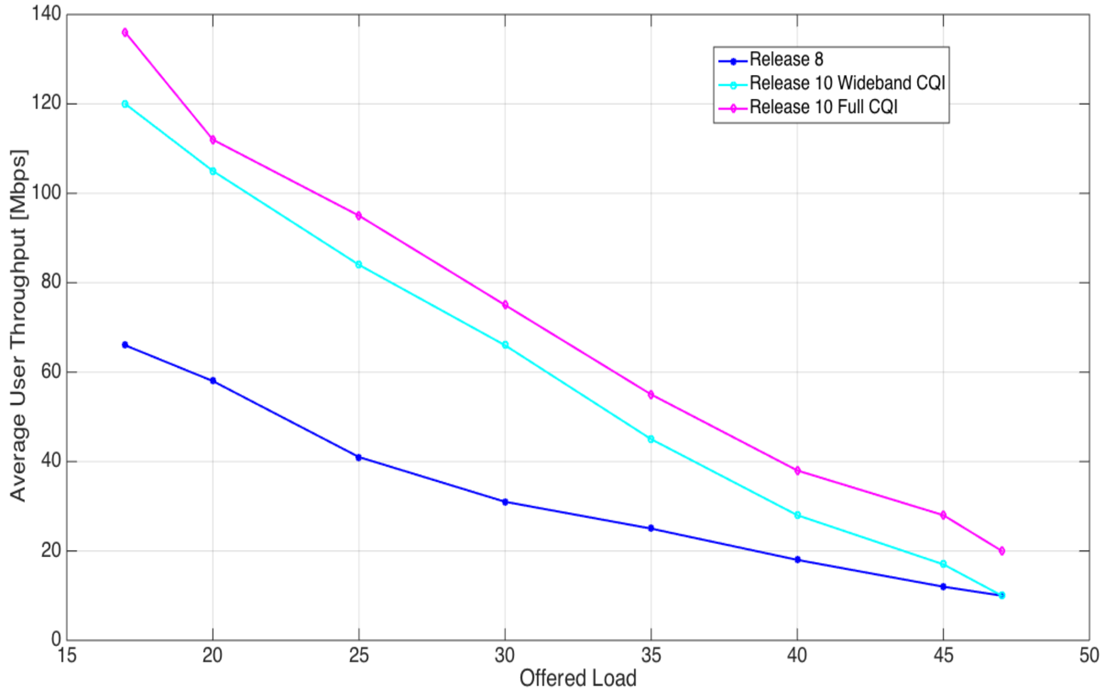

Figure 4.4: Downlink carrier Aggregation average cell performance [73]

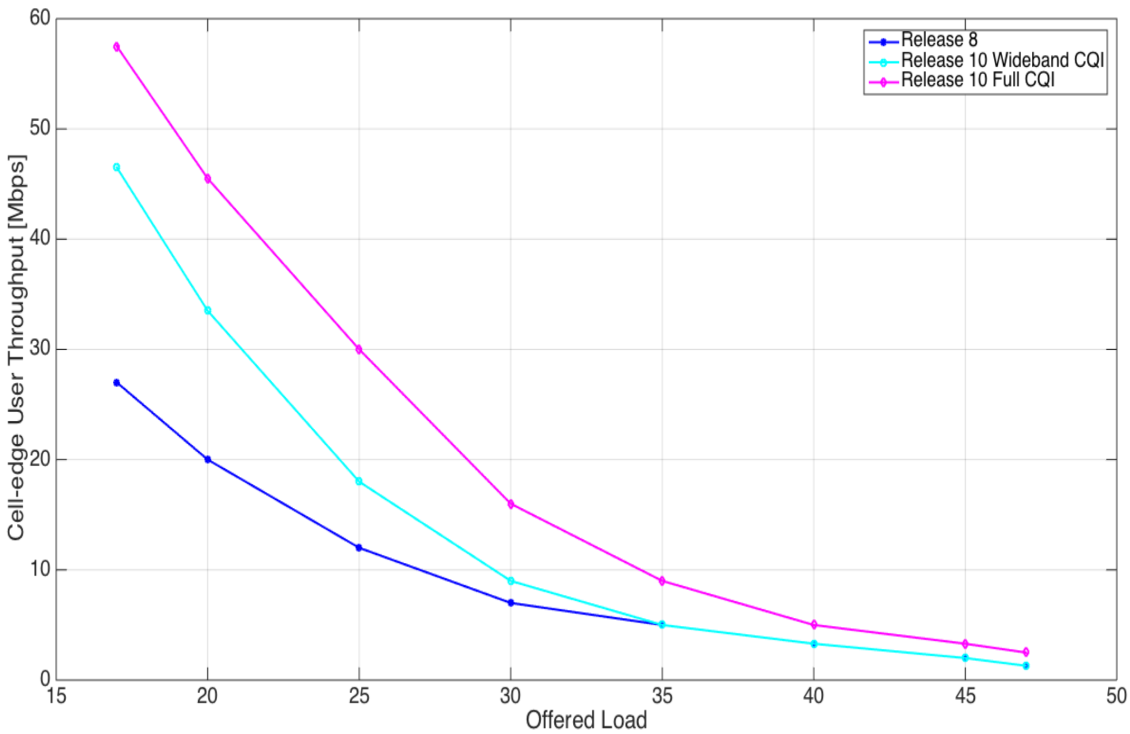

Figure 4.5: Downlink carrier Aggregation cell edge performance [73]

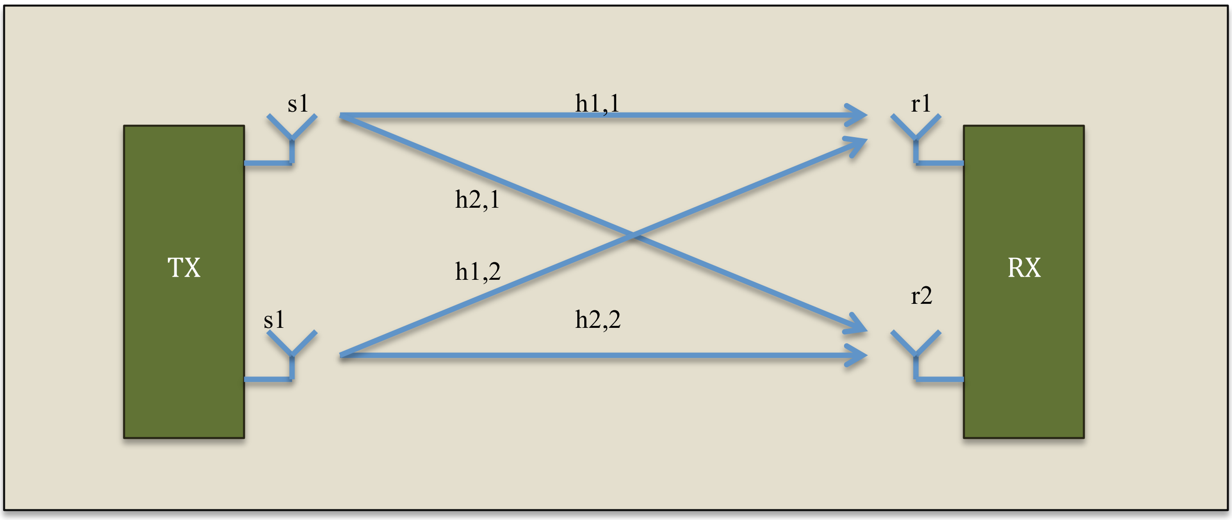

Figure 4.6: 2x2 MIMO spatial diversity antenna configuration

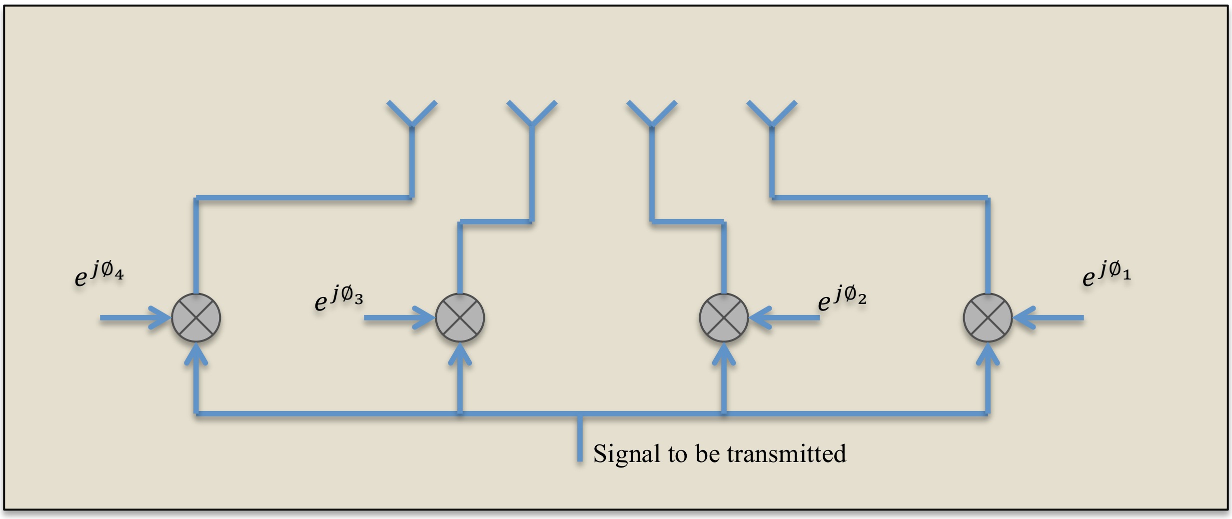

Figure 4.7: MIMO beamforming antenna configuration

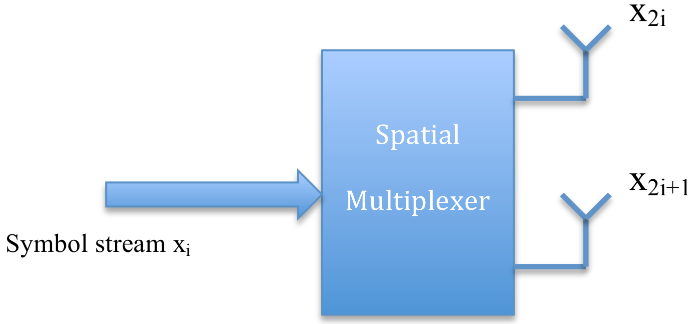

Figure 4.8: MIMO spatial multiplexing with two antennas configuration

simultaneously increased. If only N_R is increased, the capacity grows logarithmically, while the capacity converges to $N_R \log P$ if only N_T is increased [81].

Thus, to improve user spectral efficiency, SM can be used. With a given bandwidth and limited power constraints, the throughput can be increased significantly using higher numbers of antennas both at transmitter and receiver.

4.3 Heterogeneous Networks (HetNets)

With all the continuous innovations in radio interface technology along with advanced signal processing, the spectral efficiency is improved to an extent that we are about to reach the theoretical Shannon capacity limits [84][85]. But to meet the future demands, we need much more than available spectral efficiency. For that, we need to improve the network efficiency along with the improvements at the radio link level [85].

Let us consider a scenario, where multiple users are sharing a macro BS. In case of congestion, the BS limits the user throughput and in worst case a blockage occurs. To avoid that bottleneck, operator needs more of the resources. Acquiring more bandwidth is regulator dependent and costs a lot. Cell splitting is another option, where operator deploys multiple macro BSs with shorter coverage. That obviously boosts both the coverage and capacity, if interference is managed, but at the expense of additional cost in macro BS deployment.

The most feasible is to densify the cell by deploying multiple low-power nodes (LPNs), including micro-BS, picocells and femtocells. This is the most cost effective solution that would provide the higher spatial frequency reuse. This scenario where multiple cells of operating on different transmission powers with overlapping geographical coverage coexist is called Heterogeneous Network (HetNet) deployment.

In a HetNet scenario, the macro-BS provides the basic coverage and seamless mobility while the small cells enhance the coverage and capacity through spatial reuse of spectrum due to their short transmission range.

These LPNs can be deployed on the same frequencies used by macro BS or using different carrier than the macro BS while the backhaul is provided through some wired medium. The different frequency deployment creates bandwidth segmentation and is highly bandwidth inefficient. With co-channel deployment, the bandwidth efficiency is improved but at the cost of interference management schemes being introduced at each of the tier. Since interference is not the scope, so it is not being discussed here but we recommend [64][84][73] and [89] to learn about ICIC/eICIC, since, it affects the full capacity gains of HetNets.

There have been some extensive studies on performance measurements on HetNets deployment [82][83][86]-[88]. Some simulated results are shared in [85] for macro–outdoor pico scenario. The capacity is almost twice for 4 picocells deployed in the macro area, without implementing the interference management scheme. This throughput is twice the macro BS only scenario and it goes to four times if interference is managed, shown in figure 4.9. It should be noted that the gain is not linear with the deployment of picocells and eICIC.

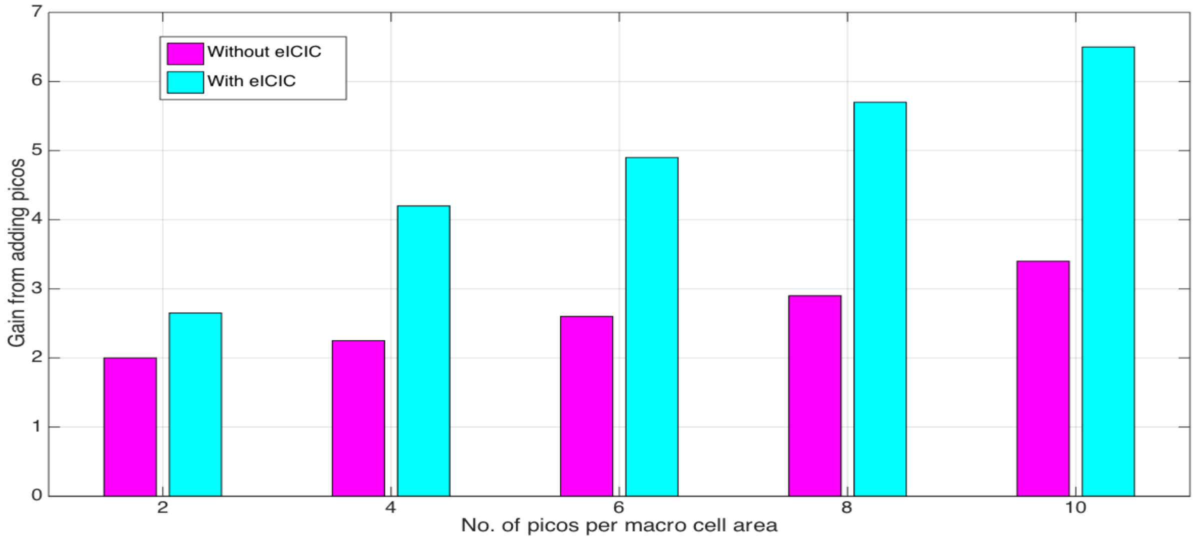

Figure 4.9: Heterogeneous Networks throughput gain [73]

This is due to the reason that for large pico deployment pico–pico interference starts to affect the performance. So, unless this interference is removed, higher gains cannot be achieved and this can be done by lowering the transmit power of these nodes. Similar results can be found in [82][83].

4.4 Relay Nodes (RNs)

Relay node (RN) is another LPN with similar specifications as a pico BS. They both have the same transmit power levels and can serve in a similar way. A major difference between the two is that an RN does not have a wired backhaul, rather it uses the same air-interface to the serving macrocell BS, called donor node, as a UE [73]. There are two types of relays:

- Amplify and Forward (AF) Relays
- Decode and Forward (DF) Relays

AF relays, commonly known as repeaters, simply amplify the incoming signal and forward it. They are used as a common tool to handle coverage holes [64][73]. But the problem is that they also amplify the incoming noise and interference, thus the SNR remains the same. Thus, they are only useful in high SNR environments.

DF relays decode and re-encode the received signal, hence eliminate the noise and interference resulting in improved SNR. Due to this property, they can be deployed even in the low SNR regions [64]. The other advantage of this relay is that the rate adaptation can be done separately on both the BS–RN and RN–UE links [73].

Furthermore, based on the backhaul spectrum usage, these relays can be categorized into In-band and Out-band relays [64][73][90]. An out-band relay uses different carrier for backhaul link than the access link. While, an in-band relay uses the same frequency band for both the backhauling and access link. The difference of resource separation for in-band and out-band relays is illustrated in figure 4.10.

During the studies, various deployment scenarios have been identified for relay technology [91]:

- Coverage extension at macro-cell edge
- Coverage hole alleviation
- User throughput enhancement
- Temporary coverage at some special event
- Service to highly mobile users (moving relays) [64][73][90]

But deploying a relay everywhere is not feasible, neither cost effective nor the performance effective. One of the main benefits of relays is that they provide homogeneous capacity to the users in the cell [92]. Since the relays use the existing resources for backhaul and also they introduce the interference, so the peak data rate of the users close to the macro-BS gets lowered but at the desired cost of improved performance at cell-edge.

There have been some studies on measuring both the capacity and coverage gains of relay deployment, mentioned in [73][92]-[95]. From those results it can be concluded that relays are more beneficial to improve coverage than the capacity. Since, the backhaul uses the same time-frequency resources, so the capacity can be increased to a certain limit. Moreover, for the same path loss, the relays perform better than macro-BSs in uplink because in downlink BSs have more power.

4.5 Coordinated Multipoint Transmission/Reception (CoMP)

LTE provides much higher peak data rates than average user-throughput and even higher than cell-edge user throughput [73]. It uses MIMO techniques to improve the average and cell-edge throughput [96]. At the cell-edge, a UE may receive signals from neighboring cells or a BS may receive signals from UEs at the cell boundaries connected to neighboring cells. If this transmission is coordinated in both ways, the performance for those edge users as well as the overall efficiency could be improved [64]. 3GPP has addressed a new spatial coordination scheme among multiple transmission/reception points, called CoMP, in Release 11 [64][97].

In general, CoMP is based on the idea of geographically distributed BSs coordinate and simultaneously transmits to a UE, especially at the border of their cells [70][73]. In this way, all the interference is turned into useful signal and can be expressed as following

$$C = B\log_2\left(1 + \frac{\sum_{i=1}^{no.of\ coordinating\ cells} S_i}{N}\right). \qquad (4.7)$$

Additionally, if BSs have the CSI, the coherent transmission can be performed which yields an extra beam-forming gain and further increases the throughput [73]. This coordination can be performed both in uplink and downlink, since the basic idea is to perform coordinated processing by BSs only. The set of BSs coordinating, both in UL and DL, is called CoMP

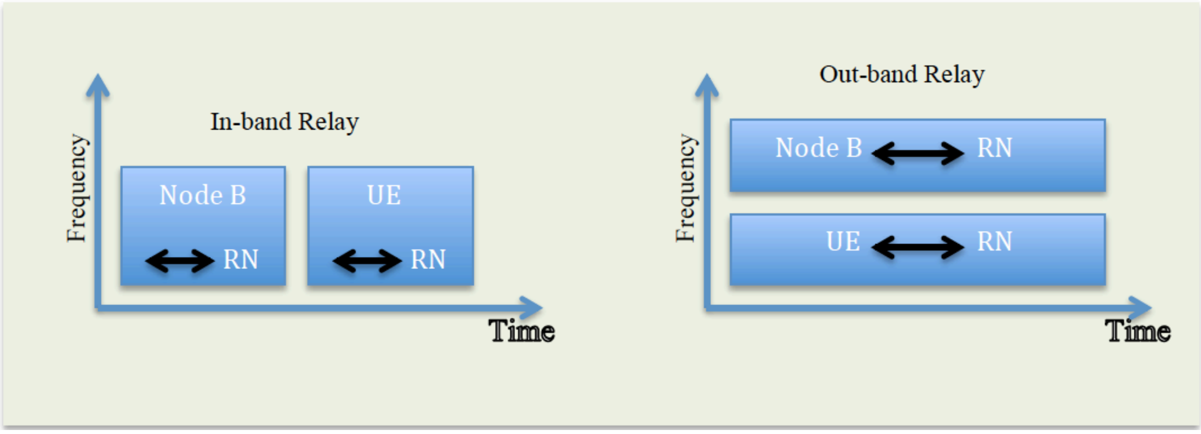

Figure 4.10: Principles of Inband and Outband relays

cooperating set and individual node is called CoMP transmission/reception point [97][99][100].

Downlink CoMP schemes can be categorized into following: [64][73][96]-[100]:

- Joint Processing (JP) where a UE data is present at multiple BSs in CoMP set
    - Joint Transmission (JT) where a subset of the CoMP set, with the UE data, simultaneously transmit to UE
    - Dynamic Point Selection (DPS) where a dynamically selected CoMP point, from CoMP set, transmits to UE; also called dynamic cell selection (DCS)
- Coordinated Scheduling/Beam-forming (CS/CB) where data is only available and transmitted by the serving point but the scheduling/beam-forming decisions are made among the set

Uplink CoMP can be categorized into followings [64][73][96]-[98]:

- Joint Reception (JR) where the data sent by UE is received by whole CoMP set
- Coordinated Scheduling/Beam-forming (CS/CB) where data is transmitted to point only but the scheduling and precoding selection decisions are made by the set

3GPP has also defined the scenarios for CoMP utilization [97]:

- Intra-site CoMP in a macrocell sectors
- Inter-site CoMP in homogeneous macrocells
- Coordination between macrocell and RRHs connected to the macro-BS
- Coordination in heterogeneous environment

There have been some results of performance evaluations of those scenarios reported in [96]-[98] and [100]. In [100], a performance comparison has been conducted for homogeneous and heterogeneous scenarios against single-cell MIMO transmission in both DCS and JT CoMP, given in table 4.1 that is taken from [100].

Table 4.1: CoMP gains, with full buffer traffic, in different scenarios under different deployment techniques [100]

		Cell average throughput gain (%)	5^{th} percentile throughput gain (%)
Macro-only deployment scenario	DCS 3 cells	0.01	6.84
	DCS 9 Cells	-0.03	10.02
	JT 3 cells	1.55	7.58
	JT 9 cells	1.25	12.68
HetNet deployment scenario	DCS 5 cells	-2.12	13.89
	DCS 15 cells	-2.15	19.28
	JT 5 cells	1.62	15.92
	JT 15 cells	1.62	23.26

Table 4.2: CoMP overall throughput gains [97][98]

	Cell average throughput gain (%)	5^{th} percentile throughput gain (%)
Downlink	4	16
Uplink	15	28

From the table 4.1, it can be observed that average throughput gain is very small. There are similar results mentioned in [73] and [96]. In [98] some of the results from [97] are mentioned, in order to avoid piracy issues only conclusion is been presented here. According to the results, CoMP brings major gains to cell-edge users both in UL and DL, as shown in table 4.2. From both the tables 4.1 and 4.2, it can be inferred that CoMP primarily acts as an interference management technique that is more useful in uplink due to receiver diversity gains.

Chapter 5

Results and Discussion

The primary objective of this work was to look for what bands are available that could be used to meet the future demands. In chapter 2, we have seen that we have three types of spectrum available. First is the primarily allocated spectrum for mobile cellular services, second are the digital dividend (DD) bands and third are the TV white spaces (TVWSs).

From table 2.1, we have seen that there are several bands available to us, especially in the mm-wavelengths that are unused. The higher bandwidths in those bands are the prospect for future. From the link budget discussion we know that with higher bandwidths we can accommodate higher data rates, which has always been the basis for future networks. But, from the same link budget calculations, we also know that these higher frequencies are prone to higher losses that limit their coverage. The important thing to note here is that capacity is related to bandwidth and with higher bandwidths the capacity is increased but the coverage is dependent on path loss, so due to bad propagation characteristics the coverage is reduced. But we know that in highly densed urban areas, the cell radius is around 200~250m; we would see in coming section whether or not this coverage requirement can be managed or not at these higher frequencies.

Other frequency bands, DDs and TVWSs, are located at lower microwave frequencies. These bands maintain their original bandwidths used for TV services. Due to their longer wavelengths, these frequencies are meant to provide basic broadband services in rural areas. Also, in table 2.2, there are some requirements that cellular services operating in TVWS bands must follow.

All these different bands were then tested on the basis of their link budget. A link budget lists all the system gains and losses. Since we are studying a large frequency spectrum, so there are some discrepancies in link budget those need to be filled. Before calculating the link budget some assumptions were made; isotropic antennas were assumed both at the BS and MS and feeder losses set to be 0dB.

In section 3.1.1, we looked at what kinds of restrictions are imposed on systems when it comes to what power they can use to transmit. Table 3.1 summarizes the numbers to avoid the adverse health effects. But these numbers are way too large to be used in a communication system due to interference issue. The communication systems use 1000s of times less power flux density. There are no power restrictions for macrocell BS but they do follow the ITU spurious emission limits. So, to avoid those emissions, the manufacturers of the system has to define the upper limit on transmit power.

So, to look at what power is actually available for different systems operating in different bands on this big spectrum, some data was collected. This data was taken from data sheets of different power amplifiers from different vendors. This data show that at higher frequencies the available power reduces, as shown in figure 3.2. This data just highlight the importance of the directive antennas and their high gain to compensate for low powers available. So, by improving the gain we can achieve the desired EIRP levels. PTS, Swedish national regulator, has defined the upper limit of 25W ERP to be used in above 47MHz bands, for mobile cellular systems. Usually, systems use 43dBm EIRP and that is the highest number used for our link budget.

Receiver sensitivity accounts for all the losses in the receiver and define *N* in SNR. It depends on both the antenna and composite-receiver temperature. Since, antenna temperature is a complex phenomenon, so it is assumed to be as reference temperature (290K). The receiver temperature is a function of composite noise figure of the receiver. The receiver is a cascaded system and composite NF depends on the gain and noise figure of the individual component of that system. The gain and noise figure of the very first component in line dominate the composite NF. So, in practice, a low noise amplifier (LNA) is put at the beginning of the chain. There is no standard relation between frequency and NF, just like transmit power, so again some numbers for NFs were collected from data sheets of different LNAs from different manufacturers. The plot in figure 3.8 shows how the NF increases with frequency due to complexity of hardware. A polynomial curve fit to actual data was also performed to model that behavior.

The channel losses play important role in determining the capacity and especially the coverage. The factors affecting the path loss and shadowing are discussed in next section. So, we are left with two important parameters that affect the SNR of the system; transmit power and receiver sensitivity.

5.1 Path Loss Exponent and Shadowing

Path loss and shadow fading are the two very important parameters. As seen in the previous chapter that atmospheric losses depend on frequency only while the path loss and shadowing define the environmental characteristics. The path loss exponent for free-space path loss model is 2 but it is not always true since LoS path is not always available as it might be the case in dense-urban environment.

Studies show that the path loss exponent varies between 4–6 for dense urban environment; as most of today's cellular systems operate under 6GHz, there exist empirical models that uses the path loss exponent for frequency term that similar to free-space model but the exponent varies in the range between 4 and 5 for distance, as in Hata and COST-231 model.

International organizations have conducted studies to develop path loss models for 5G-communication network [39] [40] [41]. ITU uses 4.342, 3GPP that is an extension to COST model uses 4.49 and WINNER also uses 4.49 the path loss exponent value. These models consider the standard deviation of shadowing to be 6dB in ITU and both 3GPP and WINNER models consider 8dB.

Moreover, there have been other studies reported in [54] where measurements were taken for path loss and shadowing, for different frequency ranges in different areas. All these studies report a path loss exponent of 2 for LoS channel. The NLoS path loss exponent for 5GHz systems varies between 3–4.5 and 3.5–5.5 for lower and higher frequencies, respectively. The shadowing reported in one study at 430MHz ranges between 3 to 6dB. The shadowing strongly depends on location, so the average shadowing at 5GHz was reported to be 7–9dB.

At 28GHz, [101] and [102], outdoor propagation measurements were conducted in New York. Both measurements show that projected cell size would be 200m in such a dense urban environment. The measurement shows that path loss exponent ranges from 5.5 to 5.7 and shadowing lies in the range 9–11dB.

At 38GHz, [103] reports the exponent 4.57 and 3.88 for peer-to-peer and cellular channel, respectively. In [104], the path loss exponent and shadowing variance for different antenna gains for clear LoS and partially obstructed non-LoS paths are compared. The path loss exponent for LoS path is similar to free-space model while the exponent is 4.17 in most obstructed NLoS path for higher gain antenna while it is 2.97 for lower gain antenna and shadowing standard deviation lies in the range 9–11dB.

In [103] and [105], measurements show that the path loss exponent in a peer-to-peer path is 4.22 and 4.19, respectively. In [106], measurements for both the backhaul and mobile scenario, the path loss exponent varies from 4.29–5.96 for mobile and 4.44–5.88 for backhaul scenario.

From all these measurement results, it is clear that at higher frequencies, due to narrow beam, mm-waves are more susceptible to path loss and shadowing. The path loss exponent varies in the range 4–6 and shadowing standard deviation is a function of location and terrain and varies in the range 7–12dB.

5.2 Cell Coverage

From equations (3.14) and (3.15), it can be seen that the cell-edge coverage can be expressed as

$$Coverage = 1 - P_{out}. \tag{5.1}$$

So, at all places in a cell at a given time, the coverage is the sum of all those places where there is no outage. This could either be temporary due to some moving object obstructing the transmission path or permanent due to UE's location behind some tree or building etc. In modern cellular services, the availability of services is maintained at 95% [15][32][36].

The coverage area calculation is not directly dependent to bandwidth, except the transmit power allocation. The MATLAB code is run for four different in-range values of RSRP set for P_{min} and figure 5.1 shows the coverage results. All the other parameters are explained and fixed in chapter 3 for different losses, the receiver noise figure is set to $12dB$ and transmit power is set to be $2\mu W/Hz$. Since, different bands have different bandwidths, so power transmitted for each band is different.

The results in the figure 5.1 matches the intuition, as the threshold limit increases the UE incurs more losses and still be able to get connectivity to the BS and also BS serves for longer distance. In blue curve there are two slopes around 600MHz that is due to the fact that these are white bands and they have low power requirements, so with higher frequency path loss increases and coverage decreases. But after 600MHz there is no low power requirement, the BS can use regular transmit power so the coverage tends to increase again. Since, blue curve is for lowest threshold limit that is why this phenomenon is visible to only this curve.

It looks great to see that by only reducing the threshold limit we can increase the coverage but it comes at a cost of expensive UE circuitry. Low threshold translates to lower UE internal noises and its efficiency to process the extremely weak received signals. Both of which is not feasible for a UE; it is supposed to be cheap but efficient. So, reducing the threshold is an option but reducing it too much is certainly not the option for operators. So, operators would need to deploy technical solutions to increase the coverage efficiency.

As in chapter 4 we studied the gains of different advanced technological solutions and some of them can be deployed to improve the coverage entirely at the cost of expenses carried by the operator. It is seen that RNs can be deployed to fill the coverage holes and provide the homogeneous capacity over the whole cell. On the other hand, CoMP increases both the average and 5^{th} percentile throughput in a cell.

From tables 4.1 and 4.2 it can be seen that CoMP gain to cell edge user is very useful to serve them better. From looking at both the RN and CoMP it can be concluded that for homogeneous capacity in a cell RN should be deployed in closer coverage hole areas and CoMP should be deployed to improve edge-user experience.

But as we know that there is a rising trend to opt for higher frequencies in the future to gain access to larger bandwidth. These higher frequencies do have large bandwidths but have very short coverage due to their propagation characteristics. So, all these higher frequencies are limited to areas where their reuse rate is high, as a result of high density of users in one place.

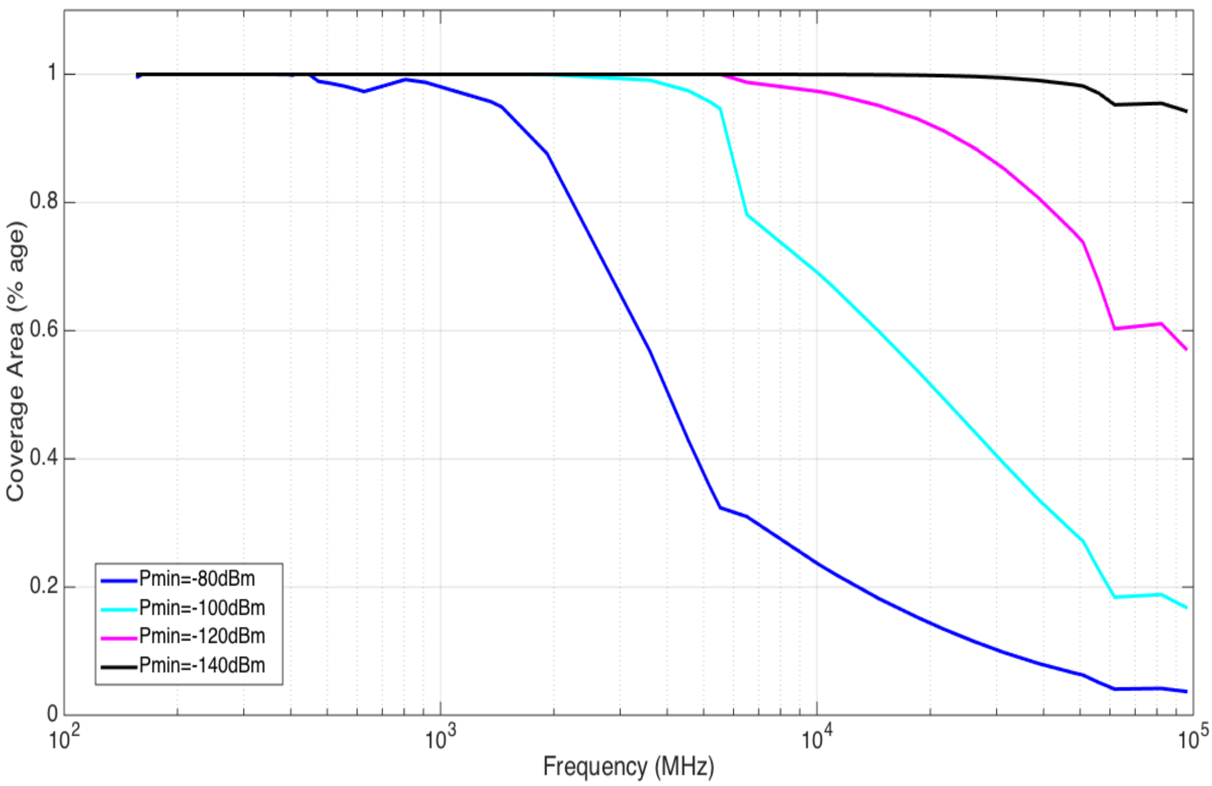

Figure 5.1: Cell coverage area vs frequency for different receiving threshold limits with different transmit powers for different carrier frequencies

Given these two requirements, these frequencies can easily be chosen for cellular services in dense urban areas. In [101] [102] [103] and [106], it is mentioned that the E-band frequencies are more feasible to only 200m radius coverage. From figure 5.2, with 95% coverage quality and cell radius of 250m, the coverage values at extremely high frequencies (EHFs), 30GHz–300GHz, satisfy the claims.

So, it can be said that higher frequencies can be deployed in highly dense area due to their inherent properties and low frequencies can be used in rural areas due to their long range. But, there is a little problem here; higher frequencies suffer more losses due to environment as well. So, just one single interruption could cause loss of connectivity to a large number of users. This problem can be avoided by the use of carrier aggregation (CA), where a low frequency carrier can be used to provide basic connectivity at all times but when user needs bandwidth for heavy data services, more bandwidth can be acquired from high carriers. With the use of RN and CoMP, this experience can be enhanced more.

5.3 User Capacity

Let us start by the following expression, from equation (4.1)

$$R \leq C = B(f)\log_2\left(1 + |h|^2 SNR(f,B)\right). \tag{5.2}$$

From equation (5.2), we know that data rate depends on the available bandwidth and the received signal power or the SNR. In general, bandwidth is fixed for an operator but in our study, we have defined both the bandwidth and SNR as a function of operating frequency. The bandwidth is variable for different frequencies and, for a given distance and receiver sensitivity, received signal power, or SNR, also depends on frequency. So, we have two parameters to improve the capacity, bandwidth linearly increases the capacity and a logarithmical increase can be done by improving SNR.

Since the need for higher data rate is growing and we cannot increase the power beyond limitations, so from table 2.1 it can be seen that larger bandwidths are available at higher frequencies that can be taken advantage of. But adopting those frequencies carelessly would cost too much; due to propagation characteristics of those frequencies propagation loss is quite large. So, for the same distance SNR would be too low as compared to lower frequencies. First, for higher frequency the signal strength will be lower and secondly the noise power at the receiver would go higher due to larger bandwidth; so reducing the overall SNR. So, in order to operate and maintain an acceptable SNR in proportionate to bandwidth at higher frequencies, large cell areas would be compromised.

Figure 5.2 shows the capacity curves, for 20MHz bandwidth system, for different distances to produce variable SNRs. It can be seen that, for a given frequency, capacity decreases as the distance increases. Since, the path loss and environmental losses are greater at higher frequencies, this effect is low at those frequencies but still can be observed.

Furthermore, to study the effects of bandwidth we fixed the path loss to 100dB, which at 95GHz translates to a distance of approximately 25m and 2.4km at 1GHz. This is done to look at how exactly the higher bandwidth availability affects the system throughput. Also, since all the available bandwidth can not be assigned to a single user due to both technical and operator resource availability restrictions, the higher bandwidths are cut off to 100MHz. Figure 5.3 shows how much capacity can be achieved by utilizing those available bandwidths at different carriers. This figure shows that under the same scenario, with more bandwidths available at higher frequencies, higher throughput can be delivered to user.

In figure 5.4, for same 100dB path loss, capacity is checked for two different bandwidths available to all carrier frequencies. This figure shows how much gain is achieved by just increasing the bandwidth. It can be seen that by increasing the bandwidth from 20 to 100MHz the capacity is increased 5-fold, which is linear to the increase in bandwidth. This figure also supports the idea of CA, discussed in previous chapter, that by aggregating more bandwidths we can achieve linear increase in capacity.

Moreover, MIMO and HetNets can also provide extended capacity gain. Current systems also use MIMO but with lower levels of MIMO; with migrating to higher frequencies could yield smaller and more antennas to build higher levels of MIMO. As we discussed in previous

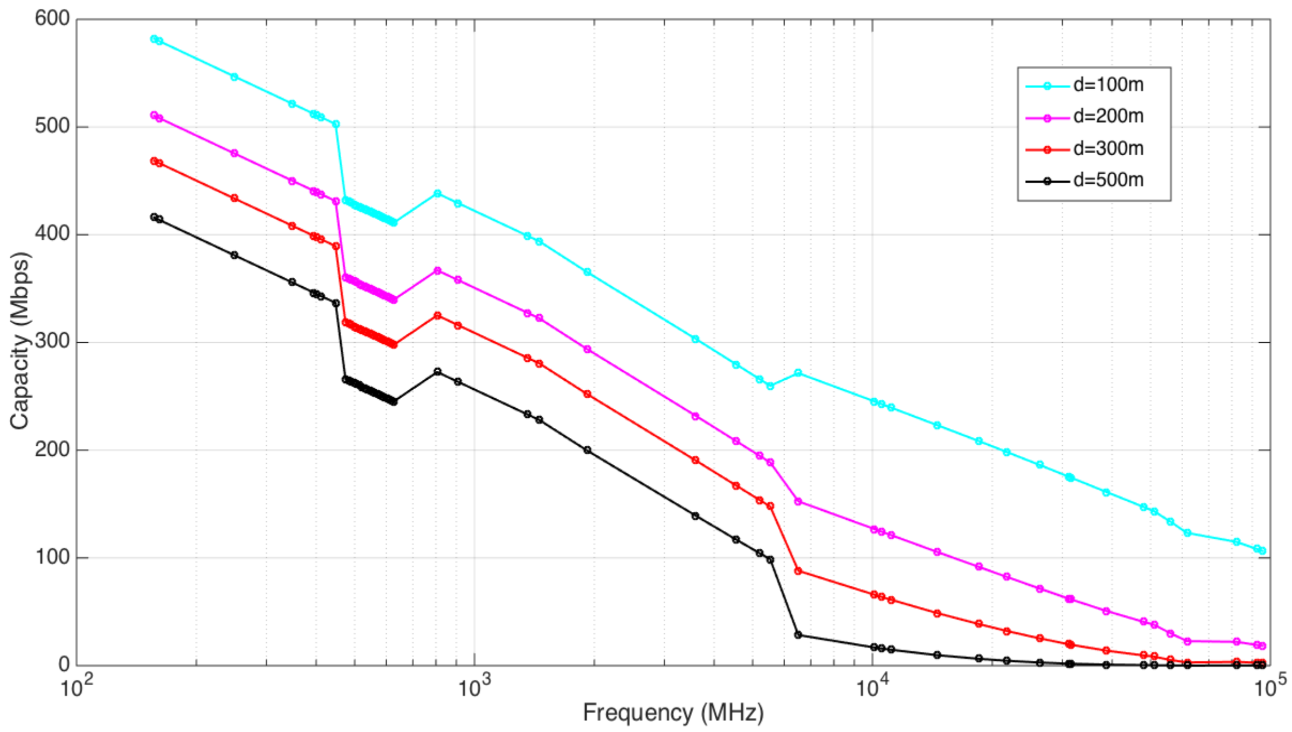

Figure 5.2: Capacity vs carrier frequency for different cell radiuses under the assumption that bandwidth is constant, i.e. 20 MHz

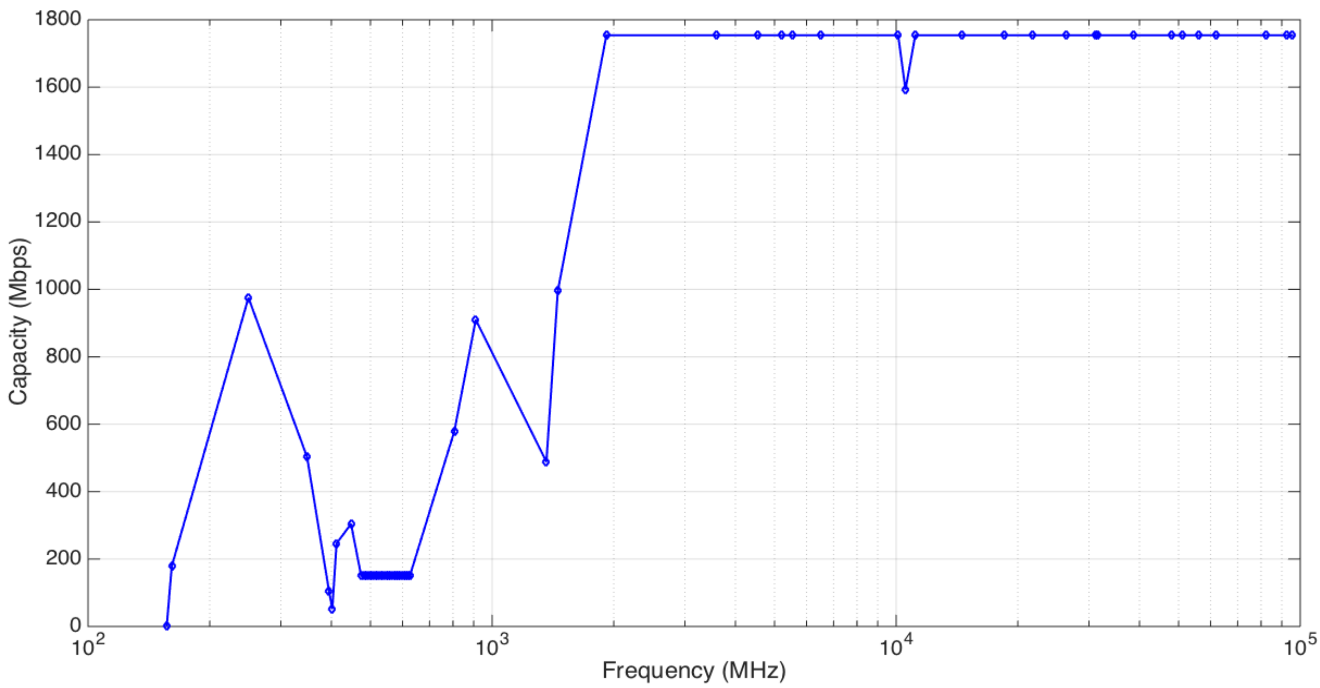

Figure 5.3: Capacity vs carrier frequency for a constant path loss, i.e. 100dB, with higher bandwidths cutoff to maximum of 100MHz

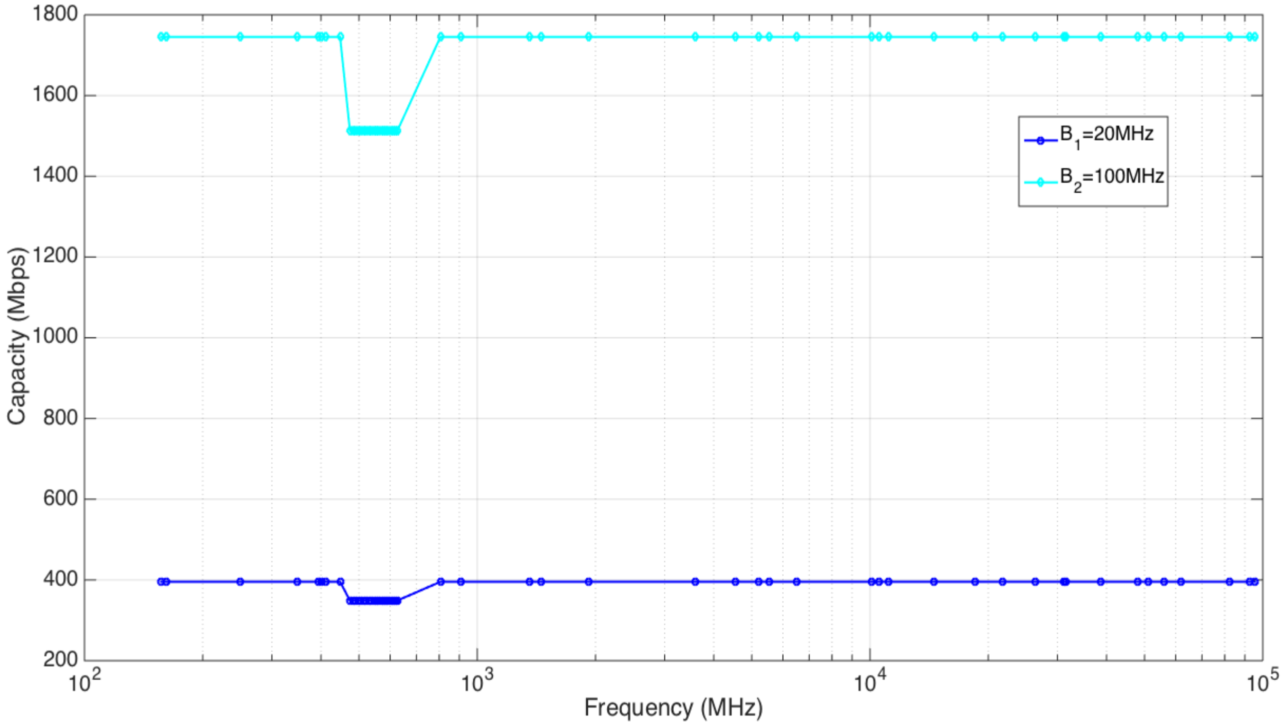

Figure 5.4: Capacity vs carrier frequency for two different sizes of bandwidths under the assumption of a constant path loss, i.e. 100dB

chapter that MIMO introduces a spatial multiplexing gain that would be higher at those higher frequencies, and HetNets with interference management can yield linear gain of 4 times with 4 pico-cell deployments. But again, one primary low carrier is needed to maintain the connectivity even in worst conditions in the cell.

So, by introducing these techniques, both the capacity and gain can be increased several fold. If, in future, a MIMO of 20x20 is implemented then by given numbers a 400-fold increase in capacity can be achieved immediately through MIMO, CA and HetNets alone. By adding CoMP and RN capacity gain, this increase would be beyond 1000-fold that is needed in future.

Conclusion

To meet the advancements and requirements of both the mobile devices and their run services, mobile networks are also getting smart. These requirements put a lot of emphasis on both the average-cell and cell-edge throughputs. Present cellular systems use the lower end of the spectrum to meet the demands. This spectrum has already reached to its full potential in terms of spectral efficiency, so it is unexpected of this spectrum to meet the 1000 fold traffic demand.

To meet those requirements, new spectrum with wide bandwidths is needed that could meet the traffic demands in near future. So, this work started by investigating what spectrum is available to use for cellular services. There are three types of bands, ITU allocated bands, digital dividends (DDs) and TV white spaces (TVWSs). Both the DD (700 and 800MHz) and TVWS (400MHz) bands are located in lower microwave frequencies, since they were previously used for terrestrial TV services. They have smaller bandwidths and certain requirements imply in the case of TVWSs. So, these bands are not feasible to be used for future traffic-heavy networks but they are good to provide basic coverage due to good propagation characteristics.

The ITU allocated bands, table 2.1, are located in both the microwave and mm-wave frequency bands. The current cellular systems use lower GHz spectrum that has shorter bandwidths but provides good coverage. From the ITU tables it can be seen that there is lots of unused spectrum, especially in the mm-wave frequencies with high bandwidths. The mm-wave frequencies hold the key to future of cellular communication as they can provide a linear increase in user throughput due to higher bandwidth availability. But this spectrum has a disadvantage, that is, higher frequencies incur more propagation losses and with higher bandwidths system noise would also be higher. To study those aspects of the system, a thorough link budget of all these frequencies is calculated.

The link budget lists all the gains and losses in a communications system. The most important parameter, to look for, is SNR. From the Shannon capacity relation, capacity depends on bandwidth and SNR. The SNR depends on transmit power, the propagations losses and the receiver noise.

Since we have assumed both the BS and MS antennas to be isotropic and feeder losses to be 1, so the EIRP depends on the transmit power. Our objective was to look for how much power in practice can be generated at transmitter and what is the allowed transmit power or EIRP and based on that what transmit power should be used in our link budget. From figure 3.2, it is seen that at higher frequencies not much power is available, probably due to complexity of hardware. But that plot shows the general trend that power generated decreases with frequency. There is no mathematical relation to show that behavior, so a polynomial curve fit is done to actual data. Generally the restrictions on transmissions are imposed on how much EIRP can be transmitted, since antenna gain and feeder losses are 0dB, so we can assume to raise the generated power levels to the allowed maximum values.

There is no maximum power limit for macrocell BSs and ITU also defines the spurious emission limits only. So, manufacturers make sure to define the maximum power such that they would not violate the spurious emission limits. Normally, 46-50dBm EIRP levels are used for transmission and PTS, the Swedish national regulator, defines the maximum 25W ERP (46dBm EIRP) to be used above 47MHz bands for cellular communications. For our work, 43dBm EIRP is used.

The channel attenuates the signal through various means, mainly the path loss and shadowing. The path loss defines the range and shadowing defines the coverage. There are different models studied in this work to choose which model to be used at what frequencies. Hata and WINNER models are used for up to 6GHz and log-distance model is used for frequencies beyond. From the study of different research works, a value of 6 for path loss component and 20m reference distance is chosen.

The received signal should be higher than the receiver internal noise in order to be decoded properly. The receiver noise depends on the noise it collects at its antenna due to surrounding and the heat produced in its circuitry. The antenna noise is assumed to be standard reference temperature (290K). The receiver noise depends on the noise figure (NF) of the receiver. The receiver noise figure is an important figure-of-merit and it depends on the gains and noise figure of the individual component. It is dominated by the gain and noise figure of the very first component; that is why in practice a low-noise amplifier (LNA) is used upfront. Different noise figure numbers from different LNAs from different manufacturers were collected to see the behavior of NF with respect to frequency, as there is no standard NF and frequency relation. The curve in figure 3.8 shows that NF increases with frequency. Since these are numbers from products used for BS, so for MS, that is cheaper, a rather higher value of 12dB is used for our link budget calculations.

From the results, it can be seen that lower frequencies provide better coverage even at very high receiving threshold while the higher frequencies can do the same but at a cost of dropping the threshold. Since, dropping the threshold all the way down is not feasible, because it would increase the complexity of a UE. So, to cover up that cost CoMP and RNs can be deployed, as they would manage the interference and coverage holes, thus providing the better coverage both in the cell and at the edge.

Since, the capacity is linearly proportional to bandwidth so by having higher bandwidths at higher frequencies increase the capacity linearly. While, this capacity is logarithmically proportional to SNR and it is observed that for a fixed distance if we decrease the SNR, capacity drop logarithmically. It is also observed that higher frequencies, due to their higher bandwidth availability, provide higher data rates but at a cost of very short distances.

So, to balance between good range and a satisfactory data rate, we need to stay in middle of the spectrum. These bands also have high data rates but to compensate higher data rates of those of higher end frequencies, we could use MIMO, CA and HetNets as they combined could produce a gain of approximately 200-400. Also, CA can be used in existing systems to combine lower and higher end frequencies to provide the advantages of both the better coverage and higher data rates, respectively.

We conclude on the point that both the lower and higher end frequencies hold an advantage over each other but to meet the future demand we need to operate on middle frequencies to compensate for good coverage at some feasible receiving threshold and good high data rates. Modern techniques can always be used to improve the gains of systems to supersede the future demands.

References

[1] ITU, *The World in 2009: ICT Facts and Figures*, ITU Telecom World 2009, Geneva, October 2009, https://www.itu.int/net/TELECOM/.../pdf/stats_ict200910.pdf

[2] ITU, *The World in 2010: ICT Facts and Figures*, World Statistics Day, October 2010, http://www.itu.int/ITU-D/ict/material/FactsFigures2010.pdf

[3] ITU, *The World in 2011: ICT Facts and Figures*, ITU World Telecom 2011, http://www.itu.int/ITU-D/ict/facts/2011/material/ICTFactsFigures2011.pdf

[4] ITU, *The World in 2013: ICT Facts and Figures*, February 2013, http://www.itu.int/en/ITU-D/Statistics/Documents/facts/ICTFactsFigures2013-e.pdf

[5] ITU, *The World in 2014: ICT Facts and Figures*, April 2014, https://www.itu.int/en/ITU-D/Statistics/Documents/facts/ICTFactsFigures2014-e.pdf

[6] Cisco, *Cisco Visual Networking Index: Global Mobile Data Traffic Forecast Update, 2010–2015*, February 2011, http://tmfassociates.com/blog/wp-content/uploads/2013/02/Cisco-mobile-VNI-Feb-2011.pdf

[7] Cisco, *Cisco Visual Networking Index: Global Mobile Data Traffic Forecast Update, 2011–2016*, February 2012, http://www.puremobile.com/media/infortis/documents/cisco_mobile_forecast.pdf

[8] Cisco, *Cisco Visual Networking Index: Global Mobile Data Traffic Forecast Update, 2012–2017*, February 2013, http://newsroom.cisco.com/.../Cisco_VNI_Mobile_Data_Traffic_Forecast_12_17.pdf

[9] Cisco, *Cisco Visual Networking Index: Forecast and Methodology, 2013–2018*, June 2014, http://www.academia.edu/9626484/Cisco_VNI_Forecast_and_Methodology_2013_18

[10] Cisco, *The Zettabyte Era: Trends and Analysis*, June 2014, http://www.slideshare.net/bytenet/the-zettabyte-era-trends-and-analysis

[11] Cisco, *Cisco Visual Networking Index: Global Mobile Data Traffic Forecast Update, 2014–2019*, February 2015, http://www.cisco.com/c/en/us/solutions/collateral/service-provider/visual-networking-index-vni/white_paper_c11-520862.html

[12] S. Nie, G. R. MacCartney, S. Sun, and T. S. Rappaport, *72 GHz Millimeter Wave Indoor Measurements for Wireless and Backhaul Communications*, in proc. IEEE 24thInt. Sym. PIMRC, September 2013, pp. 2429-2433

[13] G. R. MacCartney, J. Zhang, S. Nie, and T. S. Rappaport, *Path LossModel for 5G Millimmeter Wave Propagation Channels in Urband Microcells*, in proc IEEE GLOBECOM, December 2013, pp. 1-6

[14] R. Baldemair et al., *Evolving Wireless Communications: Addressing the Challenges and Expectations of the Future*, IEEE Vehic. Tech Mag., Vol. 8, No. 1, March 2013, pp. 24-30

[15] METIS Deliverable D1.1, *Scenarios, Requirements and KPIs for 5G Mobile and Wireless System*, April 2013, https://www.metis2020.com/wp-content/uploads/deliverables/METIS_D1.1_v1.pdf

[16] METIS Deliverable D5.1, *Intermediate Description of the Spectrum Needs and Usage Principles*, August 2013, https://www.metis2020.com/wp-content/uploads/deliverables/METIS_D5.1_v1.pdf

[17] J. W. Berresford, *The Scarcity Rationale for Regulating Traditional Broadcasting: An Idea Whose Time has Passed*, FCC Media Bureau Staff Research Paper, March 2005

[18] Post&Telestyrelsen, *General Guidelines of the Swedish National Post and Telecom Agency (PTSFS 2005:4) on the Swedish Frequency Allocation Table*, August 2005, http://www.pts.se/upload/documents/en/swedish_frequency_plan_ptsfs_2005_4.pdf

[19] ITU, *Worrld Radiocommunication Conference 2015 (WRC-15) – Agenda and Relevant Resolutions*, https://www.itu.int/dms_pub/itu-r/...PDFE.pdf

[20] GSMA, *Digital Dividend Toolkit*, Section 1.4 Auction Summary, http://www.gsma.com/spectrum/.../auctions-summary.html

[21] ITU News and Analysis Mason, *The Second Digital Dividend: Another Bite for Mobile*, https://itunews.itu.int/En/3744-The-second-digital-dividend...

[22] J. Escribiano, *Contrasting the Digital Dividend Situation in Sweden with the Rest of Europe*, March 2011, http://www.fiercewireless.com/europe/story/.../2011-03-16

[23] S. Ibrahim, *Decision About Licences to use Radio Transmitters in 791-821/832-862 MHz Frequency Band*, PTS Spectrum Department, March 2011, http://www.pts.se/upload/beslut/radio/2011/desicion-assignment-800mhz.pdf

[24] R. A. Saeed and S. J. Shellhammer, *TV White Space Technologies: Regulations, Standards and Applications*, CRC Press 2011, ISBN: 978-1-4398-4879-1

[25] Electronic Communication Committee (ECC), *PLT, DSL, Cable Communications (Including Cable TV), Lans and Their Effects on Radio Services*,, ECC Report 24, May 2003, http://www.erodocdb.dk/Docs/doc98/official/pdf/ECCREP024.PDF

[26] Electronic Communication Committee (ECC), *Technical and operational Requirements for the Possible Operation of Cognitive Radio Systems in the 'White Spaces' of the Frequency*

Band 470-790 MHz, ECC Report 159, January 2011, http://www.erodocdb.dk/Docs/doc98/official/pdf/ECCREP159.PDF

[27] Electronic Communication Committee (ECC), *Complementary Report to ECC Report 159 – Further Definition of Technical and Operational Requirements for the Operation of White Space Devices in the Band 470-790 MHz*, ECC Report 185, January 2013, http://www.erodocdb.dk/Docs/doc98/official/pdf/ECCREP185.PDF

[28] B. Sklar, *Digital communications – Fundamentals and Applications*, 2nd edition, Printice Hall PTR, , Jan 2001, ISBN: 0130847887

[29] IEEE Internation Committee on Electromagnetic Safety (SCC39), *IEEE Standard for Safety Levels with Respect to Human Exposure to Radio Frequency Electromagnetic Fields, 3 kHz to 300 GHz*, IEEE Std C95.1™-2005, April 2006

[30] ICNIRP, *ICNIRP Guidelines for Limiting Exposure to Time-Varying Electric, Magnetic and Electromagnetic Fields (up to 300 GHz)*, ICNIRP Publications – 1998, Published in Health Physics 74 (4):494-522; 1998

[31] ITU-R SM.329-12, *Unwanted Emissions in the Spurious Domain*, SM series, Recommendation, September 2012, https://www.itu.int/dms_pubrec/itu-r/rec/sm/R-REC-SM.329-12-201209-I!!PDF-E.pdf

[32] ETSI TS 136 104, *LTE; Evolved Universial Terrestrial Radio Access (E-UTRA); Base Station (BS) Radio Transmission and Reception (3GPP TS 36.104 version 12.7.0 Release 12)*, Ver. 12.7.0, April 2015, http://www.etsi.org/deliver/etsi_ts/136100_136199/136104/12.07.00_60/ts.pdf

[33] 3GPP TS 36.104, *Evolved Universal Terrestrial Radio Access (E-UTRA); Base Station (BS) Radio Transmission and Reception*, Ver. 12.7.0, March 2015, http://www.3gpp.org/dynareport/36104.htm

[34] 3GPP TS 36.101, *Evolved Universal Terrestrial Radio Access (E-UTRA); User Equipment (UE) Radio Transmission and Reception*, Ver. 12.7.0, March 2015, http://www.3gpp.org/dynareport/36101.htm

[35] ETSI TS 136 101, *LTE; Evolved Universial Terrestrial Radio Access (E-UTRA); User Equipment (UE) Radio Transmission and Reception (3GPP TS 36.101 version 12.7.0 Release 12)*, Ver. 12.7.0, May 2015, http://www.etsi.org/deliver/etsi_ts/136100_136199/136101/12.07.00_60/ts.pdf

[36] METIS Devilverable D6.1, *Simulation Guidelines*, October 2013, https://www.metis2020.com/wp-content/uploads/deliverables/METIS_D6.1_v1.pdf

[37] A. Goldsmith, *Wireless Communications*, Cambridge University Press, , 2005, ISBN: 0521837162

[38] T. S. Rappaport, *Wireless Communications – Principles and Practice*, 2nd edition, Prentice Hall PTR, 2002, ISBN: 0130422320

[39] Report ITU-R M.2135-1, *Guidelines for Evaluation of Radio Interface Technologies for IMT-Advanced*, December 2009, https://www.itu.int/.../R-REP-M.2135.pdf

[40] ETSI TR 125 996, *Universal Mobile Telecommunications System (UMTS); Spatial Channel Model for Multiple Input Multiple Output (MIMO) Simulations (3GPP TR 25.996 version 12.0.0 Release 12)*, September 2014, http://www.etsi.org/deliver/etsi_tr/125900_125999/.../tr_125996v120000p.pdf

[41] J. Meinilä, P. Kyösti, L. Hentilä, T. Jämsä, E. Suikkanen, E. Kunnari and M. Narandzic, *D5.3: WINNER+ Final Channel Models*, June 2010, http://projects.celtic-initiative.org/winner+/WINNER+%20Deliverables/D5.3_v1.0.pdf

[42] V. Erceg, L. J. Greenstein, S. Y. Tjandra, S. R. Parkoff, A. Gupta, B. Kulic, A.A. Julius and R. Bianchi, *AnEmpirically based Path Loss Model for Wireless Channels in Suburban Environments*, IEEE Journal on Selected Areas in Communications, pp. 1205-1211, July 1999

[43] S. Y. Seidel, T. S. Rappaport, S. Jain, M. L. Lord and R. Singh, *Path Loss, Scattering and Multipath Delat Statistics in Four European Cities for Digital Cellular and Microcellular Radiotelephone*, IEEE Trans. Vehic. Technology, Vol VT-40, pp. 721-730, November 1991

[44] Recommendation ITU-R P.676-10, *Attenuation by Atmospheric Gases*, September 2013, http://www.itu.int/dms_pubrec/itu-r/rec/p/R-REC-P.676-10.pdf

[45] Recommendation ITU-R P.838-3, *Specific Attenuation Model for Rain for Use in Prediction Methods*, 2005, http://www.itu.int/.../R-REC-P.838-3.pdf

[46] Recommendation ITU-R P.840-6, *attenuation due to Clouds and Fog*, September 3013, http://www.itu.int/dms_pubrec/itu-r/rec/p/R-REC-P.840-6.pdf

[47] L. J. Ippolito, *Satellite Communications Systems Engineering – Atmospheric Effects, Satellite Link Design and System Performance*, Wiley Publications, ISBN: 9780470725276

[48] S. R. Saunders, *Antennas and Propagation for Wireless Communication Systems*, Wiley Publications, 1999, ISBN: 0471986097

[49] W. C. Jakes, *Microwave Mobile Communications*, New York: Wiley, 1974, Reprinted by IEEE Press

[50] G. Stuber, *Principles of Mobile communications*, 2nd edition, Boston: Kluwer Academic Press

[51] J. E. Berg, R. Bownds, and F. Lotse, *Path loss and Fading Models for Microcells at 900 MHz*, Vehic. Technol. Conf. Rec., pp. 666-671, May 1992

[52] A. J. Goldsmith and L. J. Greenstein, *A Measurement-Based Model for Predicting Coverage Areas of Urban Microcells*, IEEE J. Selected Areas Commun., Vol. SAC-11, No. 7, pp. 1013-1023, September 1993

[53] M. Gudmundson, *Correlation Model for Shaowing in Mobile Radio Systems*, Electr. Lttrs., Vol. 27, pp. 2145-2146

[54] P. Kyösti, J. Meinilä, L. Hentilä, X. Zhao, T. Jämsä, C. Schneider, M. Narandzic, M. Miloojevic, A. Hong, J. Ylitalo, V.-M. Holappa, M. Alatossava, R. Bultitude, Y. de Jong and T. Rautiainen, *WINNER II Channel Models*, IST-4-027756 WINNER II, D1.1.2 v1.0, September 2007

[55] A. Algans, K. I. Pedersen, P. E. Mogensen, *Experimental Analysis of the Joint Statistical Properties of Azimuth Spread, Delay Spread and Shadow Fading*, IEEE J. Selected Areas in Comm., Vol. 20, pp. 523-531, 2002

[56] S. R. Saunders, *Antennas and Propagation for Wireless Communication Systems*, Wiley Publications, 1999, ISBN: 0471986097

[57] Y. Oda, R. Tsuchihashi, K. Tsunekawa, M. Hata, *Measured Path Loss and Multipath Propagation Characteristics in UHF and Microwave Frequency Band for Urban Mobile Communications*, VTC 2001 Spring, Vol. 1, pp. 337-341, 2001

[58] Y. Okumura, E. Ohmori, T. Kawano and K. Fukuda, *Field Strength and its Variability in VHF and UHF Land Mobile Radio Service*, Review of the Electrical Communication Laboratories, 16, 825-873, 1968

[60] J. Li, A. Bose and Y. Q. Zhao, *Rayleigh Flat Fading Channels' Capacity*, CNSR Conference 2005, pp. 214-217, May 2005

[61] P. M. Shankar, *Fading and Shadowing in Wireless Systems*, Springer Science and Business Media, 2012, ISBN: 9781461403678

[62] S. Atapattu, C. Tellambura and H. Jiang, *Represntation of Composite Fading and Shadowing Distribution by using Mixtures of Gamma Distributions*, WCNC 2010, pp. 1-5, April 2010

[63] A. Abdi and M. Kaveh, *K Distribution: An Appropriate Substitute for Rayleigh-Lognormal Distribution in Fading-Shadowing Wireless Channels*, Electronic Letters, Vol. 34, pp. 851-852, April 1998

[64] E. Dahlman, S. Parkvall and J. Sköld, *4G: LTE/LTE-Advanced for Mobile Broadband*, 2nd edition, Academic Press, 2014, ISBN: 9780124199859

[65] V. Jungnickel, K. Manolakis, W. Zirwas, B. Panzner, V. Barun, M. Lossow, M. Sternad, R. Apelfröjd and T. Svensson, *The Role of Small Cells, Coordinated Multipoint, an Massive MIMO in 5G*, IEEE communication Magazine, Vol. 52, pp. 44-51, May, 2014

[66] E. Hossain and M. Hasan, *5G Cellular: Key Enabling Technologies and Research Challenges*, IEEE Instrumentation & Measurement Magazine, Vol. 18, pp. 11-21, June 2015

[67] W. H. Chin, Z. Fan and R. Haines, *Emerging Technologies and Research Challenges for 5G Wireless Networks*, IEEE Wireless Communication, Vol. 21, pp. 106-112, April 2014

[68] Report ITU-R M.2134, *Requirements Related to Technical Performance for IMT-Advanced Radio Interface(s)*, 2008, https://www.itu.int/dms_pub/itu-r/opb/rep/R-REP-M.2134-2008-PDF-E.pdf

[69] R. Ratasuk, d. Tolli and A. Ghosh, *Carrier Aggregation in LTE-Advanced*, IEEE 71st Veh. Tech. Conference, pp. 1-5, May 2010

[70] G. Yuan, X. Zhang, W. Wang and Y. Yang, *Carrier Aggregation for LTE-Advanced Mobile Communication Systems*, IEEE Comm. Magzine, Vol. 48, pp. 88-93, February 2010

[71] Z. Shen, A. Papasakellariou, J. Montojo, D. Gerstenberger, F. Xu, *Overview of 3GPP LTE-Advanced Carrier Aggregation for 4G Wireless Communications*, IEEE Comm. Magzine, Vol. 50, pp. 122-130, February 2012

[72] A. Z. Yonis, M. F. L. Abdullah and M. F. Ghanim, *Effective Carrier Aggregation on the LTE-Advanced Systems*, International Journal of Advanced Science and Technology, Vol. 41, April 2012, http://www.sersc.org/journals/IJAST/vol41/2.pdf

[73] H. Harri, A. Toskala, *LTE Advanced: 3GPP Solutions for IMT-Advanced*, 1st edition, John Wiley & Sons Ltd. Publication, August 2012, ISBN: 9781119974055

[74] 3GPP TR 36.808, *Evolved Universal Terrestril Radio Access (E-UTRA); Caarier Aggregation; Base Station (BS) Radio Transmission and Reception*, Ver. 10.1.0, July 2013

[75] M. Iwamura, K. Etemad, M.-H. Fong, R. Nory and R. Love, *Carrier Aggregation Framework in 3GP LTE-Advanced [WiMAX/LTE Update]*, IEEE Comm. Magzine, Vol. 48, August 2010

[76] N. Miki, M. Iwamura, Y. Kishiyama, U. Anil, H. Ishii, *CA for Bandwidth Extension in LTE-Advanced*, NTT DOCOMO Technical Journal, Vol. 12, September 2010, https://www.nttdocomo.co.jp/.../technical_journal/bn/vol12_2/vol12_2_010en.pdf

[77] I. Shayea, M. Ismail, R. Nordin, *Capacity Evaluation of Carrier Aggregation Techniques in LTE-Advanced Systems*, 2012 Interntional Conf. on Computer and Comm. Engineering (ICCCE), pp. 99-103, July 2012

[78] K. I. Pedersen, F. Frederiksen, C. Rosa, H. Nguyen, L. G. U. Garcia and Y. Wang, *Carrier Aggregation for LTE-Advanced: Functionality and Performance Aspects*, IEEE Comm. Magzine, Vol. 49, pp. 89-95, June 2011

[79] E. Biglieri, R. Calderbank, A. Constantindies, A. Paulraj, H. V. Poor, *MIMO Wireless Communication*, Cambridge University Press, 2007, ISBN 0-521-87328-2

[80] S. Sun, T. S. Rappaport, R. W. Heath, A. Nix, *MIMO for Millimeter-Wave Wireless Communications: BEamforming, Spatial Multiplexing, or Both?*, IEEE Comm. Magzine, Vol. 52, pp-110-121, December 2014

[81] E. Telatar, *Capacity of Multi-Antenna Gaussian Channels*, European Trans. On Telecom. ETT, Vol. 10, pp-585-596, November 1999

[82] N. Bhushan, J. Li, D. Malladi, R. Gilmore, D. Brenner, A. Damnjanovic, R. Sukhavasi, C. Patel and S. Geirhofer, *Network Densification: The Dominant Theme for Wireless Evolution into 5G*, IEEE Comm. Mag., Vol. 52, pp. 82-89, February 2014

[83] A. Ghosh, N. Mangalvedhe, R. Ratasuk, B. Mondal, M. Cudak, E. Visotsky, T. A. Thomas, J. G. Andrew, P. Xia, H. S. Jo, H. S. Dhillon and T. D. Novlan, *Heterogeneous Cellular Networks: From Theory to Practice*, IEEE Comm. Mag., Vol. 50, pp. 50-64, June 2012

[84] A. Damnjanovic, J. Montojo, Y. Wei, T. Ji, M. Vajapeyam, T. Luo, T. Yoo, O. Song and D. Malladi, *A Survey on 3GPP Heterogeneous Networks*, IEEE Wireless Comm., Vol. 18, pp. 10-21, June 2011

[85] R. Q. Hu and Y. Qian, *Heterogeneous Cellular Networks*, John Wiley & Sons Ltd. 2013, ISBN: 9781119999126

[86] A. Khandekar, N. Bhushan, J. Tingfang and V. Vanghi, *LTE-Advanced: Hetereogeneous Networks*, European Wireless Conference, pp. 978-982, April 2010

[87] S. Brueck, *Heterogeneous Networks in LTE-Advanced*, International Symposium on Wireless Communication Systems (ISWCS), pp. 171-175, November 2011

[88] N. Himayat, S.-P. Yeh, A. Y. Panah, S. Talwar, M. Gerasimenko, S. Andreev and Y. Koucheryavy, *Multi-Radio Heterogeneous Networks: Architecture and Performance*, Internationsal Conf. on Computing Net. And Comm. Pp. 252-258, February 2014

[89] D. Lopez-Perez, I. Guvenc, G. de la Roche, M. Kountouris, T. Q. S. Quek and J. Zhang, *Enhanced Intercell Interference Coordination Challenges in Heterogeneous Networks*, IEEE Wirless Comm., Vol. 18, pp. 22-30, June 2011

[90] S. Yi, S. Chun, Y. Lee, S. Park and S. Jung, *Radio Protocols for LTE and LTE-Advanced*, 1st edition, John Wiley & Sons Publication, August 2012, ISBN: 9781118188538

[91] M. Iwamura, H. Takahashi and S. Nagata, *Relay Technologies in LTE-Advanced*, NTT DOCOMO Technical Journal, Vol. 12, September 2010, https://www.nttdocomo.co.jp/.../technical_journal/bn/vol12_2/vol12_2_029en.pdf

[92] T. Beniero, S. Redana, J. Hamalainen and B. Raaf, *Effect of Relaying on Coverage in 3GPP LTE-Advanced*, IEEE 69th Vehicular Tech. Conference, pp. 1-5, April 2009

[93] R. Schoenen, W.Zirwas and B. H. Walke, *Capacity and Coverage Analysis of a 3GPP-LTE Multihop Deployment Scenario*, IEEE International Conference on Comm. Workshops, pp. 31-36, May 2008

[94] A. B. Saleh, S. Redana, J. Hamalainen and B. Raaf, *On the Coverage Extension and Capacity Enhancement of Inband Relay Deployments in LTE-Advance Networks*, journal of Electrical and Computer Engineering, Vol. 2010, May 2010, http://www.hindawi.com/journals/jece/2010/894846/

[95] A. B. Saleh, S. Redana, B. Raaf and J. Hamalainen, *Comparison of Relay and Pico eNB Deployments in LTE-Advanced*, 2009 IEEE 70th Vehicular Tech. Conference, pp. 1-5, September 2009

[96] S. Ahmadi, *LTE-Advanced: A Practical System Approach to Understanding 3GPP LTE Release 10 and 11 Radio Access Technologies*, Academic Press, 2014, ISBN: 9780124051621

[97] 3GPP TR 36.819, *Technical Specification Group Radio Access Network; Coordinated Multi-point Operation for LTE Physical Layer Aspects*, Ver. 11.2.0, September 2009

[98] A. Elnashar, M. A. El-saidny and M. R. Sherif, *Design, Deployment and Performance of 4G-LTE Networks: A practical Approach*, Jhn Wiley & Sons, 2014, ISBN: 9781118683217

[99] J. Acharya, L. Gao and S. Gaur, *Heterogeneous Networks in LTE-Advanced*, John Wily & Sons, 2014, ISBN: 9781118511862

[100] B. Mondal, E. Visotsky, T. A. Thomas, X. Wang and A. Ghosh, *Performance of Downlink CoMP in LTE under Practical Constraints*, IEEE 23rd International Symposium on Personal Indoor and Mobile Radio Communications (PIMRC), pp. 2049-2054, September 2012

[101] Y. Azar, G.N. Wong, K. Wang, R. Mayzus, J. K. Schulz, H. Zhao, F. Gutierrez, D. Hwang and T. S. Rappaport, *28 GHz Propagation Measurements for Outdoor Cellular Communications using Steerable Beam Antennas in New York City*, IEEE International Conference on Communications (ICC), pp. 5143-5147, June 2013

[102] M. Samimi, K. Wang, Y. Azar, G. N. Wong, R. Mayzus, H. Zhao, J. K. Schulz, S. Sun, F. Gutierrez and T. S. Rappaport, *28 GHz Angle of Arrival and Angle of Departure Analysis for Outdoor Cellular Communications usingSteerable Beam Antennas in New York City*, IEEE 77th Veh. Tech. Conference, pp. 1-6, June 2013

[103] T. S. Rappaport, E. Ben-Dor, J.N. Murdock and Y. Qiao, *38 GHz and 60 GHz Angle-Dependent Propagation for Cellular & Peer-to-Peer Wireless Communications*, IEEE International Conference on Communications (ICC) pp. 4568-4573, June 2012

[104] T. S. Rappaport, F. Gutierrez, E. Ben-Dor, J. N. Murdock, Y. Qiao and J.I. Tamir, *Broadband Millimeter-Wave Propagation Measurements and Models using Adaptive-Beam Antennas for Outdoor Urban Cellular Communications*, IEEE Trans. On Antenna and Propagation, pp. 1850-1859, April 2013

[105] E. Ben-Dor, T. S. Rappaport, Y. Qiao and S. J. Lauffenburger, *Millimeter-Wave 60 GHz Outdoor and Vehicle AoA Propagation Measurements using a Broadband Channel Sounder*, IEEE Global Telecomm. Conference, pp. 1-6, December 2011

[106] G. R. MacCartney, T. S. Rappaport, *73 GHz Millimeter Wave Propagation Measurements for Outdoor Urban Mobile and Backhaul Communications in New York City*, IEEE International Conference on Comm. (ICC), pp. 4862-4867, June 2014